Controlling nano- and microfilament morphology by strategically placing chiral centers in the side chains of bent-core molecules

Ashwathanarayana Gowda, Gourab Acharjee, Suraj Kumar Pathak, Grace A.R. Rohaley, Asmita Shah, Robert P. Lemieux, Marianne E. Prévôt* and Torsten Hegmann*

Electronic Supplementary Information (ESI)

Section S1. Synthesis and Analytical Data

1. Materials and General Methods

All chemicals and starting materials were purchased from Sigma-Aldrich, Fisher Scientific, or VWR. Organic solvents used in the reactions were dried and distilled using standard protocols prior to use. Reactions were monitored by thin layer chromatography (TLC, Merck KGaA). Crude compounds were purified using a CombiFlash NextGen 300 flash chromatography system with UV detection (Teledyne ISCO, Inc. Lincoln, NE, USA) using W. R. Grace & Co. silica gel cartridges. All glassware used for the reactions were cleaned and dried overnight at 140 °C in an oven.

2. Analytical Methods

The molecular structure and purity of all intermediate and final compounds were established by spectroscopic and mass spectrometric methods. ^{1}H NMR (nuclear magnetic resonance) spectra were recorded using a Bruker Avance at 400 MHz and ^{13}C NMR at 100 MHz using deuterated chloroform ($CDCl_3$) as a solvent. Chemical shifts (δ) are given in parts per million (ppm) relative to tetramethylsilane (TMS) as an internal standard. ^{1}H NMR: δ = 7.23 ppm; ^{13}C NMR: δ = 77.0 ppm). The patterns (splitting or multiplicity) of the ^{1}H NMR signals are represented as *s* = singlet, *d* = doublet, *t* = triplet, *dd* = doublet of doublet, *dt* = doublet of triplet, *m* = multiplet and coupling constants (*J*) are given in Hz. High-resolution mass spectrometry was performed at Indiana University's mass spectrometry laboratory using either a Thermo MAT-95 high resolution magnetic sector mass spectrometer (ESI source) or a Waters LCT with LockSpray ESI source for accurate mass analysis.

3. Synthesis

The syntheses of intermediate compounds **12c–d**, **13c–d**, **14c–d**, **15c–d** have been reported previously by our group. Details about these previously synthesized intermediate compounds can be found in the following literature: references (S1) – (S4).

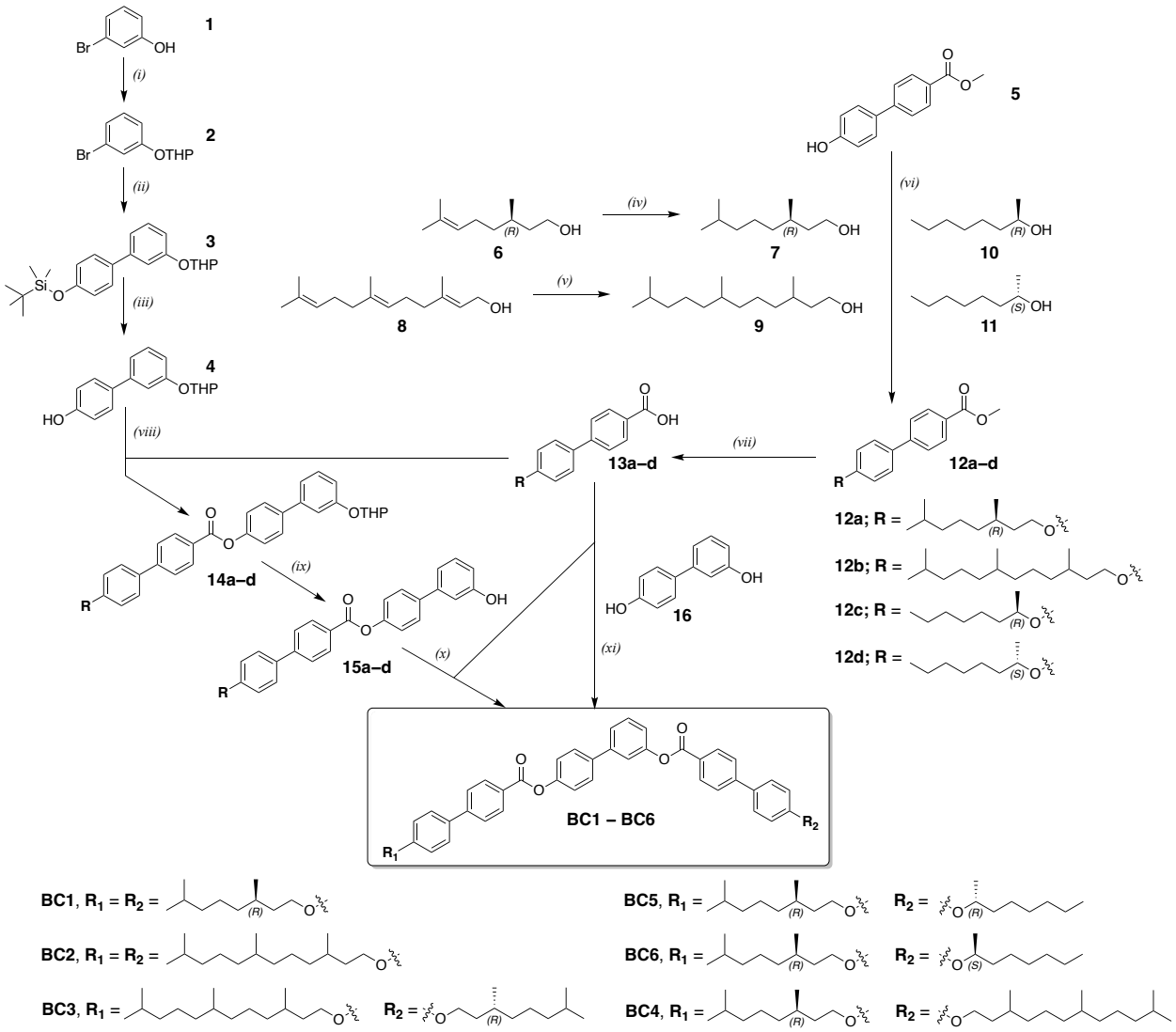

Scheme S1. Synthesis scheme of final bent-core molecules (BC1 – BC6). The synthesis methods of intermediate compounds have been reported previously **(1–4)**. (*i*) DHP, PTSA, DCM, r.t., 3 h; (*ii*) 4-(*tert*-butyldimethylsilyloxy)phenylboronic acid, $Pd(PPh_3)_4$, 2M Na_2CO_3, benzene, reflux, 12 h; (*iii*) Bu_4NF, THF, r.t., 12 h; (*iv*) Pd/C, EtOAc, r.t., 24 h; (*v*) Pd/C, EtOAc, r.t., 48 h; (*vi*) alkanol, TPP, DIAD, dry THF, r.t., >3 h; (*vii*) $LiOH \cdot H_2O$, MeOH: H_2O (7:3), reflux, 12 h; (*viii*) EDCI, DMAP, DCM:THF (1:1), r.t., 12 h; (*ix*) conc. HCl, DCM, r.t., 12 h; (*x*) EDCI, DMAP, DCM:THF (1:1), r.t., 12 h; (*xi*) EDCI, DMAP, DCM:THF (1:1), r.t., 24 h; (r.t. = room temperature, DHP = dihydropyran, PTSA = *p*-toluenesulfonic acid, DCM = dichloromethane, TPP triphenylphosphine, DIAD = diisopropyl azodicarboxylate, EDCI = 1-ethyl-3-(3-dimethylaminopropyl)carbodiimide, DMAP = dimethylaminopyridine).

3.1. Synthesis of (R)-3,7-dimethyloctan-1-ol (7)

(*R*)-3,7-dimethyloct-6-en-1-ol (1 g, 6.4 mmol) was placed in a single necked round bottom flask along with 20 mL dry ethyl acetate. The reaction mixture was degassed by bubbling argon

for 10 mins. Immediately after, activated 5% Pd/C catalyst (140 mg) was added to the reaction mixture. The reaction mixture was stirred at room temperature in presence of a hydrogen atmosphere for 12 h. After completion, the reaction mixture was filtered through a celite pad, and the residue was thoroughly washed with ethyl acetate. The filtrate was concentrated under reduced pressure to obtained (*R*)-3,7-dimethyloctan-1-ol (**7**) as a colorless oil (1.0 g, quantitative). The crude compound was used for the next step without further purification. ^{1}H NMR ($CDCl_3$, 400 MHz, *δ*/ppm): *δ* 3.76–3.61 (m, 2H, OCH_2), 1.69–1.47 (m, 2H), 1.44–1.18 (m, 8H), 0.99–0.76 (m, 9H, $3CH_3$). ^{13}C NMR ($CDCl_3$,100 MHz, *δ*/ppm): *δ* 61.17 (C–O), 40.02, 39.94, 37.51, 32.79, 29.53, 27.98, 24.81, 22.73, 19.66.

3.2. Synthesis of 3,7,11-trimethyldodecan-1-ol (9)

3,7,11-trimethyldodecan-1-ol **(9)** was synthesized following the procedure described above for compound **7**. Quantities: farnesol **8** (1 g, 4.5 mmol), 5 wt.% Pd/C catalyst (220 mg) and stirred for 48 h under a hydrogen atmosphere. The final product **9** was a colorless oil (1.1 g, quantitative). The crude compound was used for the next step without further purification. ^{1}H NMR ($CDCl_3$, 400 MHz, *δ*/ppm): *δ* 3.75–3.65 (m, 2H, OCH_2), 1.68–1.48 (m, 3H), 1.44–1.22 (m, 10H), 1.18–1.06 (m, 4H), 0.94–0.83 (m, 12H, $4CH_3$). ^{13}C NMR ($CDCl_3$,100 MHz, *δ*/ppm): *δ* 61.24 (C–O), 40.03, 39.37, 37.50, 37.46, 37.33, 32.79, 29.53, 27.99, 24.83, 24.38, 22.73, 22.64, 19.75, 19.62.

3.3. Synthesis of (R)-methyl 4'-((3,7-dimethyloctyl)oxy)-[1,1'-biphenyl]-4-carboxylate (12a)

To a stirring solution of compound **5** (0.5 g, 2.19 mmol) in dry THF (20 mL) was added triphenylphosphine (PPh_3) (0.746 g, 2.85 mmol) and (*R*)-3,7-dimethyl-1-octanol **7** (0.381 g, 2.41 mmol) under a nitrogen atmosphere. The resulting reaction mixture was allowed to stir at 0 °C for 10 minutes. To this, diisopropyl azodicarboxylate (DIAD) (0.575 g, 2.85 mmol) in 3 mL dry THF was added dropwise under nitrogen flow. The resulting reaction mixture was magnetically stirred in an ice bath for 5 hours. The reaction was monitored by thin layer chromatography (TLC). After completion of the reaction, the reaction mixture was washed with brine solution and extracted with dichloromethane (DCM; 3 × 50 mL). The combined extracts were dried over Na_2SO_4, and solvent was evaporated under vacuum. The crude compound was taken to the next step without further purification (yield: 0.68 g, 85%).

3.4. Synthesis of methyl 4'-((3,7,11-trimethyldodecyl)oxy)-[1,1'-biphenyl]-4-carboxylate (12b)

Compound **12b** was synthesized following the procedure described for compound **12a**. Quantities: compound **5** (1 g, 4.38 mmol), 3,7,11-trimethyldodecan-1-ol **(9)** (1.1 g, 4.82 mmol), PPh_3 (1.49 g, 5.70 mmol), DIAD (1.15 g, 5.70 mmol.) The crude product **(12b)** was taken to the next step without further purification (yield: 1.67 g, 87%).

3.5. Synthesis of (R)-4'-((3,7-dimethyloctyl)oxy)-[1,1'-biphenyl]-4-carboxylic acid (13a)

A mixture of compound **12a** (1.5 g, 4.07 mmol) and lithium hydroxide monohydrate (1.71 g, 40.73 mmol) was dissolved in a mixture of methanol / water (40 mL) (7:3 = *v*:*v*). The resultant reaction mixture was refluxed at 80 °C for 12 h. After completion of the reaction, the reaction mixture was cooled to r.t. and subsequently quenched with concentrated hydrochloric acid (HCl, ~ 37%) to adjust the pH ~ 2. The resulting material was collected by vacuum filtration, washed with excess of water, and dried in a vacuum oven overnight to obtain white solid (yield = 1.37 g, 95%). ^{1}H NMR ($CDCl_3$, 400 MHz, δ/ppm): δ 8.18 (d, J = 8.5 Hz, 2H, biphenyl), 7.69 (d, J = 8.5 Hz, 2H, biphenyl), 7.61 (d, J = 8.5 Hz, 2H, biphenyl), 7.02 (d, J = 8.5 Hz, 2H, biphenyl), 4.12–4.03 (m, 2H, OCH_2), 1.94–1.82 (m, 1H), 1.77–1.56 (m, 3H), 1.42–1.14 (m, 6H), 0.99 (d, J = 6.5 Hz, 3H, CH_3), 0.93–0.87 (m, 6H, $2CH_3$). ^{13}C NMR ($CDCl_3$,100 MHz, δ/ppm): δ 171.38 (C=O), 159.56, 146.19, 132, 130.78, 128.41, 127.15, 126.56, 114.98, 77.24, 66.48, 39.26, 37.30, 36.18, 29.87, 28, 24.69, 22.74, 22.63, 19.68.

3.6. Synthesis of 4'-((3,7,11-trimethyldodecyl)oxy)-[1,1'-biphenyl]-4-carboxylic acid (13b)

Compound **13b** was synthesized following the procedure described for compound **13a**. Quantities: compound **12b** (0.4 g, 0.91 mmol), lithium hydroxide monohydrate (0.38 g, 9.12 mmol), methanol / water (20 mL) (7:3 = *v*:*v*). The final product was a white solid (yield: 0.36g, 95%). ^{1}H NMR ($CDCl_3$, 400 MHz, δ/ppm): δ 8.19 (d, J = 8.5 Hz, 2H, biphenyl), 7.69 (d, J = 8.5 Hz, 2H, biphenyl), 7.61 (d, J = 8.8 Hz, 2H, biphenyl), 7.02 (d, J = 8 Hz, 2H, biphenyl), 4.12–4.03 (m, 2H, OCH_2), 1.92–1.85 (m, 1H), 1.75–1.55 (m, 3H), 1.44–1.06 (m, 14H), 0.99 (d, J = 6.5 Hz, 3H, CH_3), 0.89 (dd, J = 6.6, 4.7 Hz, 9H, $3CH_3$). ^{13}C NMR ($CDCl_3$, 100 MHz, δ/ppm): δ 171.79 (C=O), 159.56, 146.20, 132, 130.78, 128.41, 127.22, 126.56, 114.98, 66.48, 39.38, 37.40, 37.33, 37.29, 36.23, 36.15, 32.81, 29.87, 28, 24.85, 24.37, 22.75, 22.65, 19.78, 19.73, 19.70, 19.67.

3.7. Synthesis of 3'-((tetrahydro-2H-pyran-2-yl)oxy)-[1,1'-biphenyl]-4-yl 4'-(((R)-3,7-dimethyl-octyl)oxy)-[1,1'-biphenyl]-4-carboxylate (14a)

In a two-neck flask containing compound **4** (0.2 g, 0.740 mmol), compound **13a** (0.288 g, 0.814 mmol) and a catalytic amount of 4-dimethylaminopyridine (DMAP) (20 mg) were added in a mixture of dry DCM and THF (1:1 = *v*:*v*) (50 mL) under argon at room temperature. After stirring for 10 min, 1-ethyl-3-(3-dimethylaminopropyl)carbodiimide (EDCI) (0.23 g, 1.480 mmol) was added. The resulting mixture was stirred at room temperature for 12 h. After completion of the reaction, water was added, and the mixture extracted with DCM (3 × 50 mL). The combined extracts were dried over Na_2SO_4 and concentrated under vacuum. The residue was purified by CombiFlash chromatography system (*n*-hexane/ethyl acetate) (9:1 = *v*:*v*) to afford a white solid **14a** (yield: 0.35 g, 80%). ^{1}H NMR ($CDCl_3$, 400 MHz, δ/ppm) δ 8.32–8.25 (m, 2H, biphenyl), 7.77–7.59 (m, 6H, biphenyl), 7.43–7.29 (m, 4H, biphenyl), 7.25 (ddd, J = 7.7, 1.8, 1.0 Hz, 1H, biphenyl), 7.13–7.00 (m, 3H, biphenyl), 5.53 (t, J = 3.3 Hz, 1H), 4.16–4.04 (m, 2H, OCH_2), 4.01–3.95 (m, 1H), 3.69–3.64 (m, 1H), 2.07 (m, 1H), 1.99–1.83 (m, 3H), 1.76–1.62 (m, 6H), 1.57–1.54 (m, 1H), 1.40–1.30 (m, 3H), 1.24–1.17 (m, 3H), 1.0 (d, J = 6.5 Hz, 3H), 0.91 (m, J = 6.7, 0.6 Hz, 6H, $2CH_3$). ^{13}C NMR ($CDCl_3$, 100 MHz, δ/ppm): δ 165.23 (C=O), 159.59, 157.50, 150.49, 146.04, 141.83, 138,82, 131.98, 130.77, 129.76, 128.42, 127.46, 126.63, 121.98, 120.50, 115.50, 115.29, 115.01, 96.46, 74.21, 66.49, 62.11, 39.27, 37.31, 36.18, 30.43, 29.87, 28.01, 25.25, 24.69, 22.74, 19.69, 18.82.

3.8. *Synthesis of 3'-((tetrahydro-2H-pyran-2-yl)oxy)-[1,1'-biphenyl]-4-yl 4'-((3,7,11-trimethyl-dodecyl)oxy)-[1,1'-biphenyl]-4-carboxylate* (14b)

Compound **14b** was synthesized following the procedure described for compound **14a** above. Quantities: compound **4** (0.2 g, 0.740 mmol), compound **13b** (0.345 g, 0.814 mmol), DMAP (20 mg), EDCI (0.229 g, 1.480 mmol) and DCM / THF (1:1 = *v*:*v*) (50 mL). The final product was a white solid (yield: 0.43 g, 87%). ^{1}H NMR ($CDCl_3$, 400 MHz, δ/ppm): δ 8.28 (d, J = 8.5 Hz, 2H, biphenyl), 7.76–7.70 (m, 2H, biphenyl), 7.65 (dd, J = 16.3, 8.7 Hz, 4H, biphenyl), 7.39 (t, J = 7.9 Hz, 1H, biphenyl), 7.35–7.29 (m, 3H), 7.26–7.22 (m, 1H, biphenyl), 7.13–7.0 (m, 3H, biphenyl), 5.53 (t, J = 3.3 Hz, 1H), 4.13–4.04 (m, 2H, OCH_2), 3.98 (ddd, J = 12.3, 9.5, 3.1 Hz, 1H), 3.69–3.64 (m, 1H), 2.13–2.00 (m, 1H), 1.97–1.83 (m, 3H), 1.78–1.63 (m, 5H), 1.55–1.50 (m, 1H), 1.42–1.08

(m, 12H), 0.99 (dd, J = 6.5, 0.7 Hz, 3H, CH_3), 0.89 (ddd, J = 6.6, 4.4, 0.7 Hz, 9H, $3CH_3$). ^{13}C NMR ($CDCl_3$, 100 MHz, δ/ppm): δ 165.23 (C=O), 159.59, 157.50, 150.49, 146.04, 141.83, 138.82, 131.98, 130.77, 129.75, 128.42, 128.28, 127.46, 126.63, 121.98, 120.50, 115.50, 115.29, 115.01, 96.46, 74.24, 66.49, 62.11, 39.38, 37.38, 37.33, 37.29, 36.23, 36.14, 32.81, 30.43, 29.87, 28, 25.25, 24.84, 24.37, 22.70, 22.65, 19.78, 19.72, 19.70, 19.67, 18.82.

3.9. *Synthesis of (R)-3'-hydroxy-[1,1'-biphenyl]-4-yl 4'-((3,7-dimethyloctyl)oxy)-[1,1'-biphenyl]-4-carboxylate* (15a)

Compound **14a** (0.25 g, 0.412 mmol) was dissolved in dry DCM (20 mL) to which conc. hydrochloric acid (37%, 250 µL) was dropwise added at room temperature. The resulting reaction mixture was stirred at room temperature for 12 h. After completion of the reaction, the reaction mixture was quenched with 2M aqueous sodium carbonate (10 mL) and extracted with DCM (3 × 30 mL). The combined extracts were dried over Na_2SO_4 and concentrated under vacuum. The residue was purified by a CombiFlash chromatography system (*n*-hexane/ethyl acetate) (9:1 = *v*:*v*) to afford a white solid **15a** (yield: 0.2 g, 95%). ^{1}H NMR ($CDCl_3$, 400 MHz, δ/ppm): δ 8.33–8.25 (m, 2H, biphenyl), 7.77–7.70 (m, 2H, biphenyl), 7.66–7.60 (m, 4H, biphenyl), 7.38–7.28 (m, 3H, biphenyl), 7.19 (dt, J = 7.8, 1.2 Hz, 1H, biphenyl), 7.10–7.00 (m, 3H, biphenyl), 6.85 (ddd, J = 8.1, 2.6, 1.0 Hz, 1H, biphenyl), 5.10 (s, 1H, OH), 4.14–4.02 (m, 2H, OCH_2), 1.94–1.86 (m, 1H), 1.76–1.55 (m, 3H), 1.41–1.17 (m, 6H), 1.00 (d, J = 6.5 Hz, 3H, CH_3), 0.91 (d, J = 6.6 Hz, 6H, 2 CH_3). ^{13}C NMR ($CDCl_3$, 100 MHz, δ/ppm): δ 165.36 (C=O), 159.60, 155.95, 150.55, 146.11, 142.13, 138.54, 131.96, 130.80, 130.06, 128.43, 128.22, 127.37, 126.65, 122.04, 119.71, 115.03, 114.32, 114.09, 74.20, 66.51, 39.27, 37.31, 36.18, 29.87, 29.73, 28.01, 24.70, 22.74, 22.64, 19.69.

3.10. *Synthesis of 3'-hydroxy-[1,1'-biphenyl]-4-yl 4'-((3,7,11-trimethyldodecyl)oxy)-[1,1'-biphenyl]-4-carboxylate* (15b)

Compound **15b** was synthesized following the procedure described for compound **15a** above. Quantities: compound **14b** (0.3 g, 0.443 mmol), conc. HCl (33%, 300 µL) and DCM (10 mL). The final product was a white solid **15b** (yield: 0.25 g, 95%). ^{1}H NMR ($CDCl_3$, 400 MHz, δ/ppm) δ 8.34–8.25 (m, 2H, biphenyl), 7.77–7.70 (m, 2H, biphenyl), 7.66–7.62 (m, 4H, biphenyl), 7.36–7.31 (m, 3H, biphenyl), 7.21–7.18 (ddd, J = 7.7, 1.7, 1.0 Hz, 1H, biphenyl), 7.09–7.00 (m, 3H, biphenyl), 6.86 (ddd, J = 8.1, 2.5, 1.0 Hz, 1H, biphenyl), 4.95 (s, 1H, OH), 4.16–4.02 (m, 2H,

OCH_2), 1.94–1.83 (m, 1H), 1.78–1.50 (m, 4H), 1.45–1.09 (m, 12H), 1.05–0.87 (m, 3H, CH_3), 0.92–0.83 (m, 9H, $3CH_3$). ^{13}C NMR ($CDCl_3$, 100 MHz, δ/ppm): δ 165.31 (C=O), 159.60, 155.91, 150.57, 146.10, 142.17, 138.52, 131.96, 130.07, 128.43, 128.22, 127.38, 126.65, 122.05, 119.76, 115.02, 114.31, 114.31, 96.46, 77.24, 66.51, 39.38, 37.38, 37.33, 37.29, 36.23, 36.15, 32.82, 29.88, 28.01, 24.84, 24.37, 22.75, 19.78, 19.74, 19.71, 19.68.

3.11. Synthesis of final compounds BC1 – BC6

All final bent-core molecules were prepared by esterification reaction between the intermediate compounds **15** and compound **16** with various alkoxy phenyl benzoic acids **13**. The general method is given below:

3.11.1. Synthesis of compound **BC1** and **BC2**

In a two neck-flask containing compound **16** (1 eq.), alkoxy phenyl benzoic acids **13a** or **13b** (2.1 eq.), and a catalytic amount of 4-dimethylaminopyridine (DMAP) (0.5 eq.) were added in a mixture of dry DCM and THF (1:1 = *v*:*v*) (10 mL) under argon at room temperature. After stirring for 10 min, 1-ethyl-3-(3-dimethylaminopropyl)carbodiimide (EDCI) (4 eq.) was added. The resulting mixture was stirred at room temperature for 24 h. After completion of the reaction, water was added, and the resulting mixture extracted with DCM. The combined extracts were dried over Na_2SO_4 and concentrated under vacuum. The residue was purified by CombiFlash chromatography instrument (*n*-hexane/ethyl acetate, 9:1 = *v*:*v*) to obtain the desired compounds **BC1** and **BC2** as white solids; yields ranging from 80% to 90%.

Compound **BC1**: ^{1}H NMR ($CDCl_3$, 400 MHz, δ/ppm): δ 8.31–8.28 (m, 4H, biphenyl), 7.75–7.69 (m, 6H, biphenyl), 7.65–7.62 (m, 4H, biphenyl), 7.56–7.54 (m, 2H, biphenyl), 7.50 (dt, J = 2.3, 1.0 Hz, 1H, biphenyl), 7.36–7.34 (m, 2H, biphenyl), 7.28–7.26 (m, 1H, biphenyl), 7.05–7.03 (m, 4H, biphenyl), 4.11–4.06 (m, 4H, $2OCH_2$), 1.93–1.85 (m, 2H), 1.74–1.52 (m, 6H), 1.40–1.17 (m, 12H), 0.99 (d, J = 6.5 Hz, 6H, $2CH_3$), 0.91 (dd, J = 6.6, 0.6 Hz, 12H, $4CH_3$). ^{13}C NMR ($CDCl_3$, 100 MHz, δ/ppm): δ 165.18 (2C=O), 159.60, 151.46, 150.76, 146.07, 142.10, 138, 131.98, 130.78, 129.87, 128.42, 128.34, 127.44, 127.40, 126.64, 124.65, 122.15, 120.69, 120.53, 115.01, 66.49, 39.26, 37.31, 36.18, 29.87, 28, 24.69, 22.74, 22.63, 19.69. HRMS. *m*/*z*: (MH^+) calcd. for ($C_{58}H_{66}O_6$): 859.4932, found: 859.4936. Spectroscopic data are shown in Fig. S1.

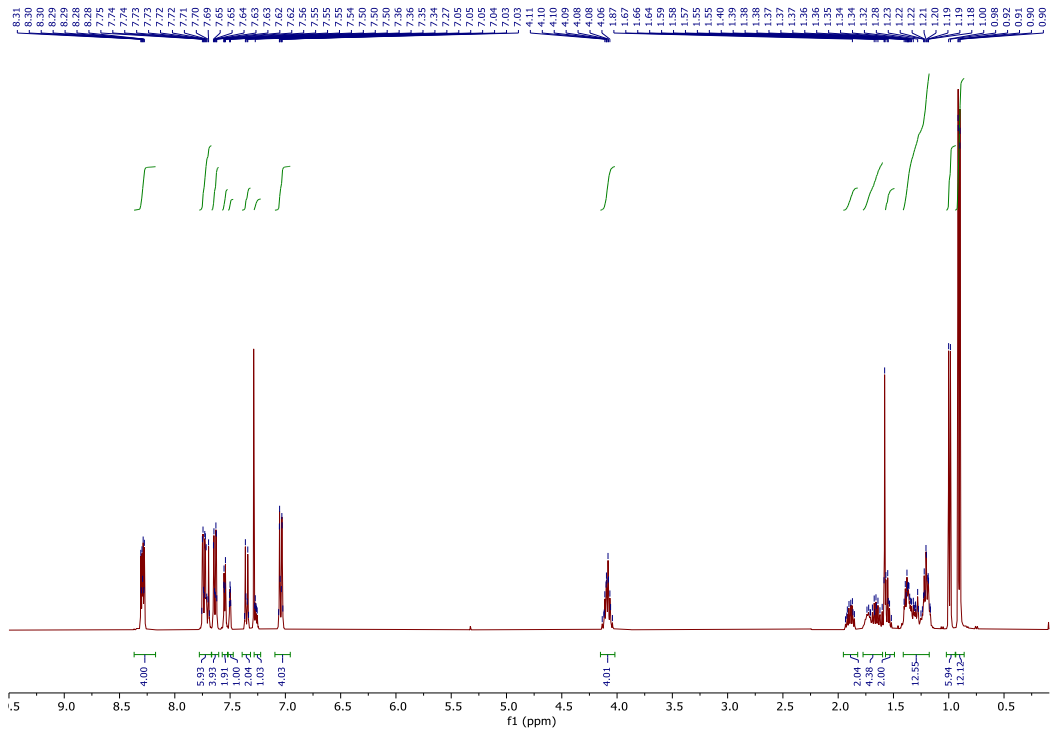
f1 (ppm)

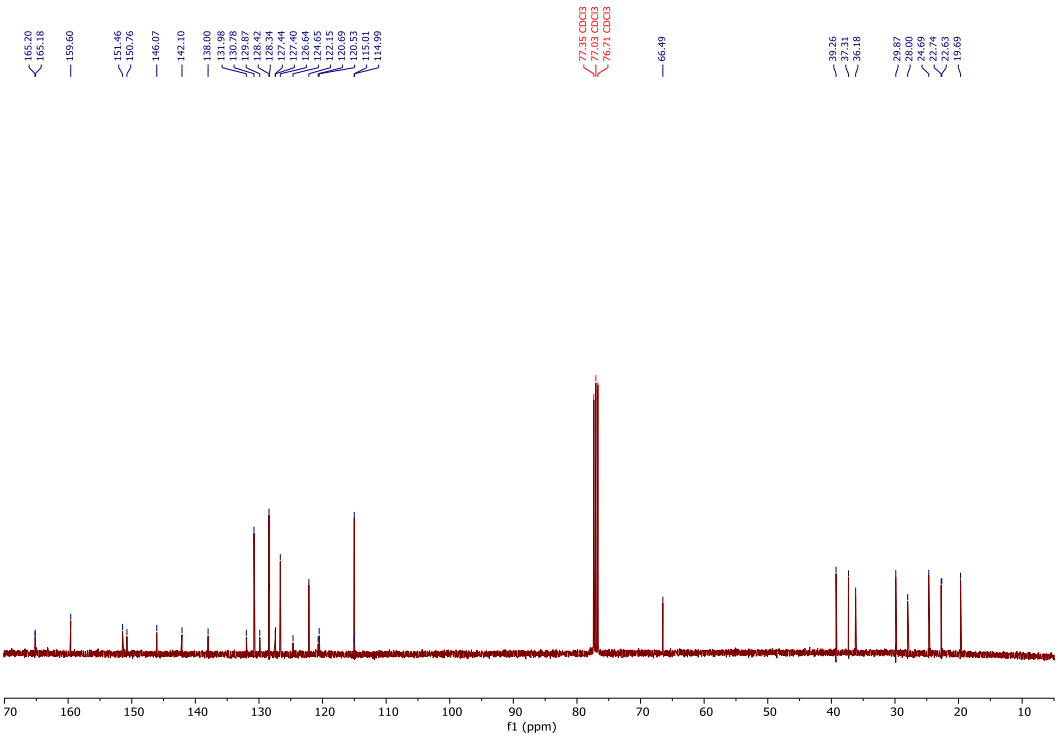
f1 (ppm)

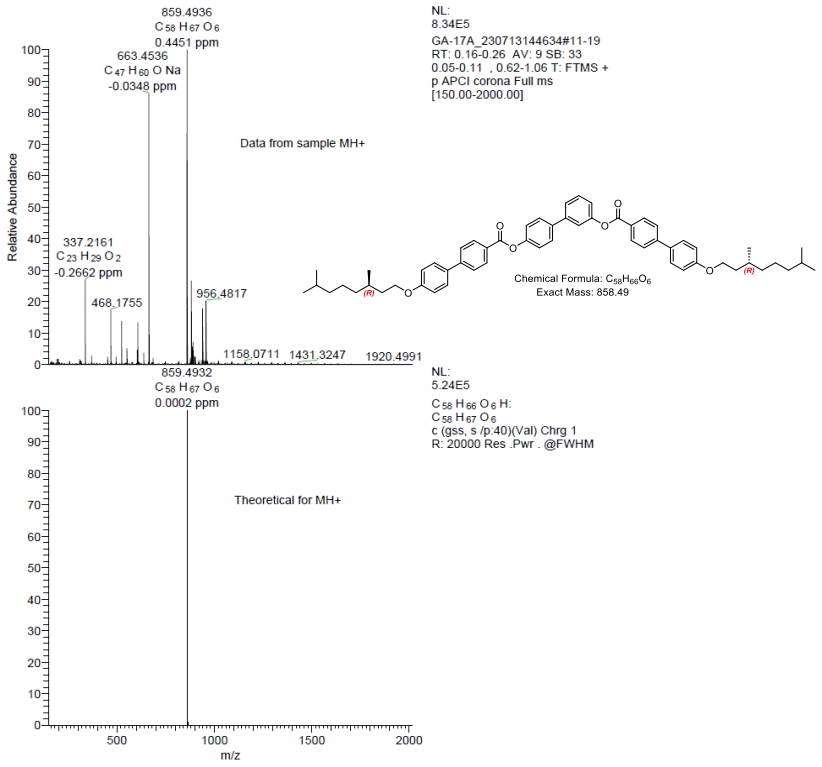

Fig. S1. ^{1}H NMR, ^{13}C NMR and HRMS spectrum of compound **BC1**.

Compound **BC2**: ^{1}H NMR ($CDCl_3$, 400 MHz, δ/ppm):): δ 8.31–8.27 (m, 4H, biphenyl), 7.76–7.69 (m, 6H, biphenyl), 7.66–7.62 (m, 4H, biphenyl), 7.56–7.54 (m, 2H, biphenyl), 7.50 (ddd, J = 2.3, 1.4, 0.8 Hz, 1H, biphenyl), 7.37–7.33 (m, 2H, biphenyl), 7.28–7.26 (m, 1H, biphenyl), 7.06–7.02 (m, 4H, biphenyl), 4.14–4.04 (m, 4H, $2OCH_2$), 1.94–1.85 (m, 2H), 1.76–1.63 (m, 4H), 1.59–1.50 (m, 2H), 1.43–1.09 (m, 26H), 1.00 (dd, J = 6.5, 0.7 Hz, 6H, $2CH_3$), 0.89 (ddd, J = 6.6, 4.4, 0.7 Hz, 18H, $6CH_3$). ^{13}C NMR ($CDCl_3$, 100 MHz, δ/ppm): δ 165.19 (2C=O), 159.60, 151.45, 150.76, 146.07, 142.10, 138, 131.97, 130.78, 129.88, 128.42, 128.34, 127.44, 127.39, 126.64, 124.65, 122.16, 120.70, 120.53, 115.01, 66.49, 39.38, 37.42, 37.40, 37.37, 37.33, 37.29, 36.24, 36.15, 32.82, 29.88, 28.01, 24.85, 24.83, 24.37, 22.76, 22.66, 19.78, 19.74, 19.71, 19.68. HRMS. m/z: (MH^+) calcd. for ($C_{68}H_{86}O_6$): 999.6497, found: 999.6503. Spectroscopic data are shown in Fig S2.

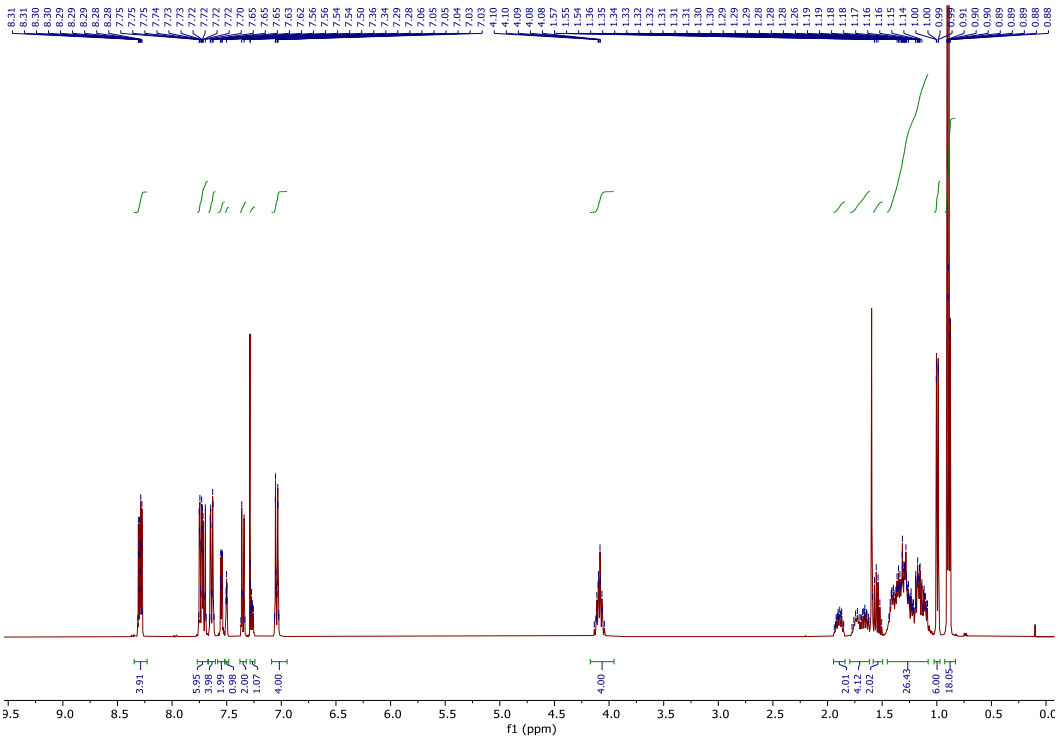
f1 (ppm)

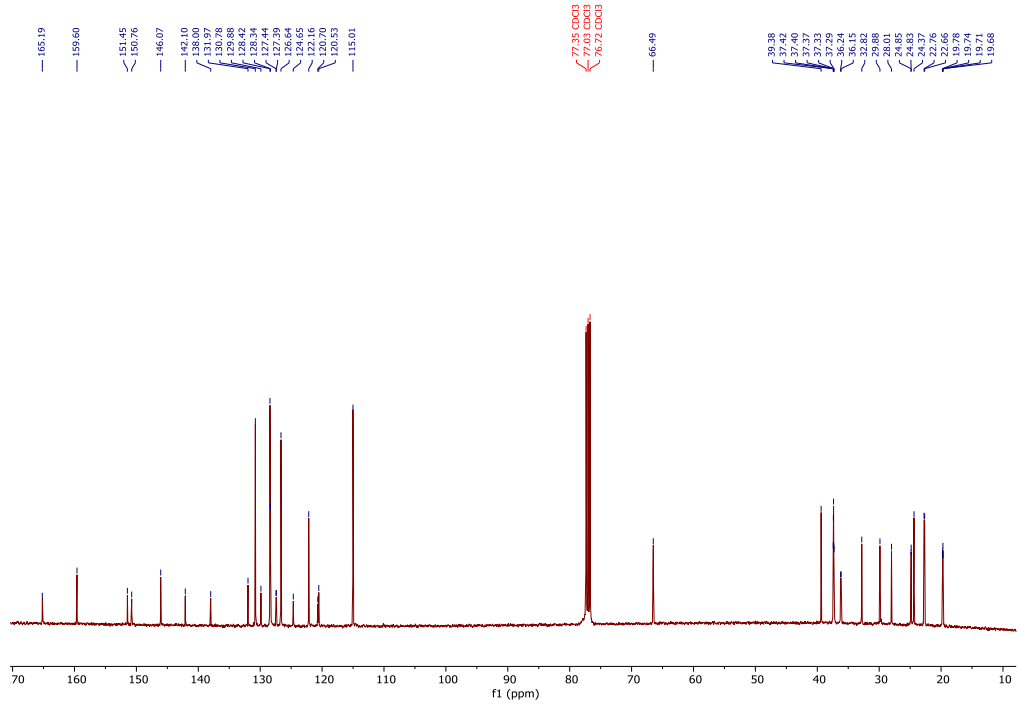
f1 (ppm)

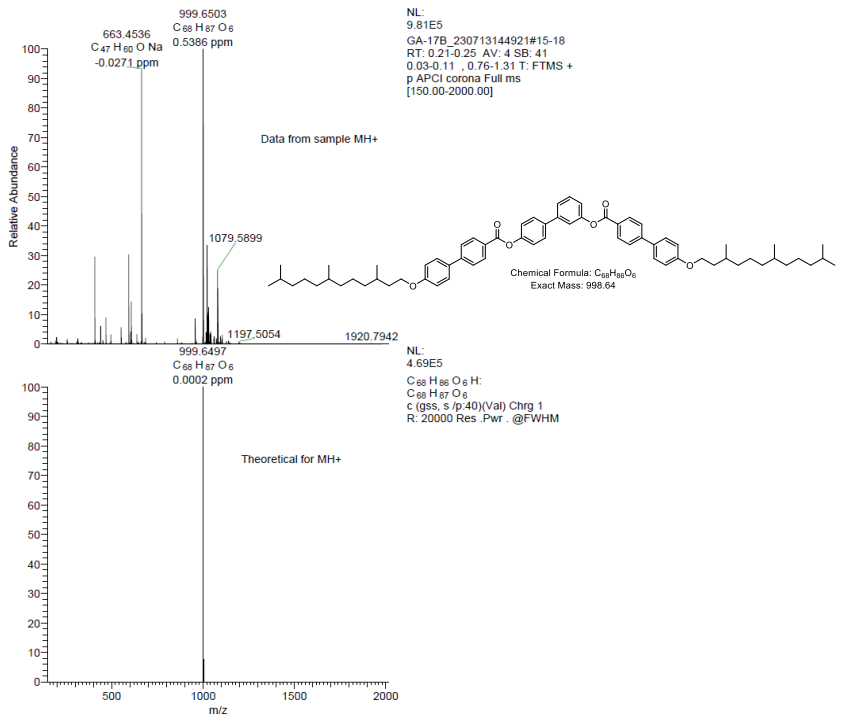

Fig. S2. ^{1}H NMR, ^{13}C NMR and HRMS spectrum of compound **BC2**.

3.11.2. Synthesis of compounds **BC3 – BC6**

Compounds **BC3 – BC6** were synthesized following the procedure described for **BC1** or **BC2** above. Quantities: specific combinations of compound **15a**, **15b**, **15c**, or **15d** (1 eq.), compound **13a**, **13b**, **13c**, or **13d** (1 eq.), DMAP (0.2 eq.), and EDCI (2 eq.). The final products were white solids; yields ranging from 80% to 90%.

Compound **BC3**: ^{1}H NMR ($CDCl_3$, 400 MHz, δ/ppm): δ 8.31–8.27 (m, 4H, biphenyl), 7.76–7.69 (m, 6H, biphenyl), 7.66–7.62 (m, 4H, biphenyl), 7.56–7.54 (m, 2H, biphenyl), 7.50 (dt, J = 2.3, 0.9 Hz, 1H), 7.37–7.33 (m, 2H, biphenyl), 7.29–7.25 (m, 1H, biphenyl), 7.06–7.02 (m, 4H, biphenyl), 4.13–4.04 (m, 4H, 2OCH_2), 1.94–1.85 (m, 2H), 1.76–1.60 (m, 4H), 1.57–1.52 (m, 2H), 1.41–1.15 (m, 19H), 0.99 (d, J = 6.5 Hz, 6H, 2CH_3), 0.90 (dtd, J = 6.6, 4.5, 0.6 Hz, 15H, 5CH_3). ^{13}C NMR ($CDCl_3$, 100 MHz, δ/ppm): δ 165.19 (2CO), 159.60, 151.46, 150.76, 146.07, 142.10, 138, 131.97, 130.78, 129.87, 128.42, 128.34, 127.44, 127.40, 126.64, 124.65, 122.15, 120.69, 120.53, 115.01, 66.49, 39.38, 39.26, 37.42, 37.38, 37.31, 37.29, 36.23, 36.19, 36.14, 32.81,

29.87, 29.73, 28.01, 24.84, 24.69, 24.37, 22.75, 22.64, 19.78, 19.74, 19.69. HRMS. *m*/*z*: (MH^+) calcd. for ($C_{63}H_{76}O_6$): 929.5715, found: 929.5720. Spectroscopic data are shown in Fig. S3.

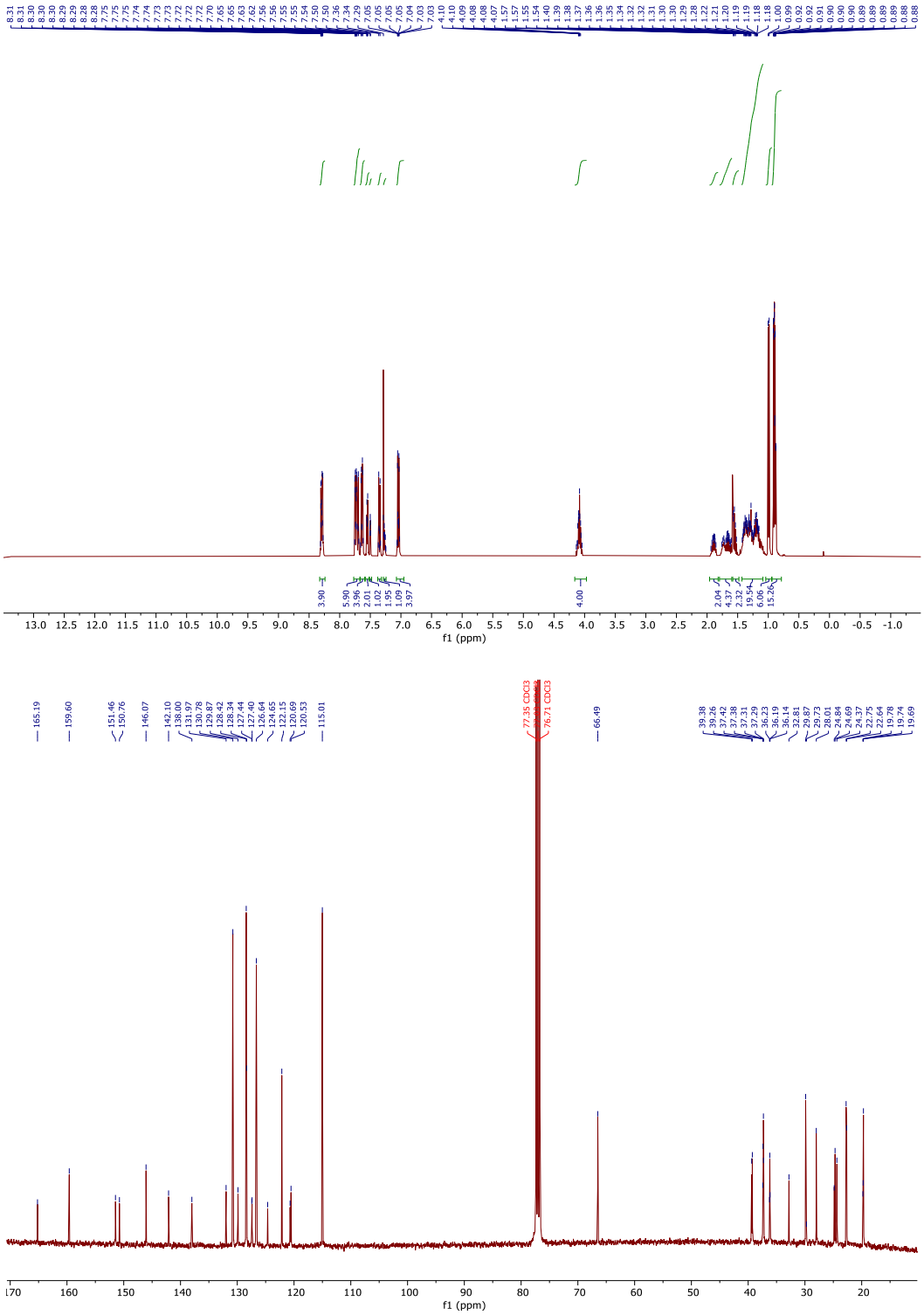

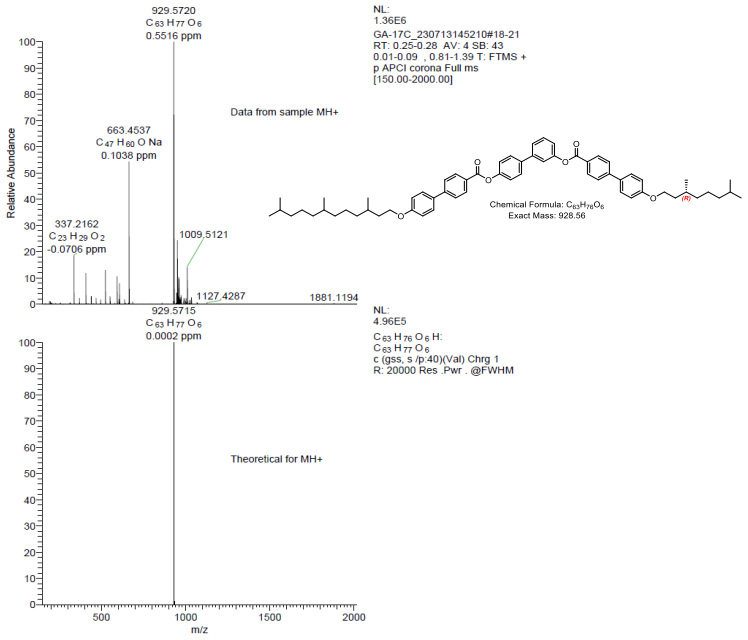

Fig. S3. ^{1}H NMR, ^{13}C NMR and HRMS spectrum of compound **BC3**.

Compound **BC4**: ^{1}H NMR ($CDCl_3$, 400 MHz, δ/ppm): δ 8.31–8.28 (m, 4H, biphenyl), 7.76–7.69 (m, 6H, biphenyl), 7.66–7.62 (m, 4H, biphenyl), 7.56–7.54 (m, 2H, biphenyl), 7.50 (dt, J = 2.2, 0.9 Hz, 1H, biphenyl), 7.37–7.33 (m, 2H, biphenyl), 7.28–7.25 (m, 1H, biphenyl), 7.06–7.02 (m, 4H, biphenyl), 4.13–4.04 (m, 4H, $2OCH_2$), 1.92–1.85 (m, 2H), 1.76–1.60 (m, 4H), 1.57–1.52 (m, 2H), 1.42–1.13 (m, 19H), 0.99 (dd, J = 6.5, 0.9 Hz, 6H, $2CH_3$), 0.92–0.88 (m, 15H). ^{13}C NMR ($CDCl_3$, 100 MHz, δ/ppm): δ 165.20 (2CO), 159.59, 151.45, 150.76, 146.07, 142.10, 138, 131.97, 130.78, 129.88, 128.42 128.34, 127.44, 127.39, 126.64, 124.65 122.15, 120.70, 120.53, 115.01, 66.49, 39.38, 39.26, 37.39, 37.31, 36.23, 36.18, 32.81, 29.87, 28.01, 24.84, 24.69, 24.37, 22.75, 22.65, 19.78, 19.74, 19.69. HRMS. m/z: (MH^+) calcd. for ($C_{63}H_{76}O_6$): 929.5715, found: 929.5719. Spectroscopic data are shown in Fig. S4.

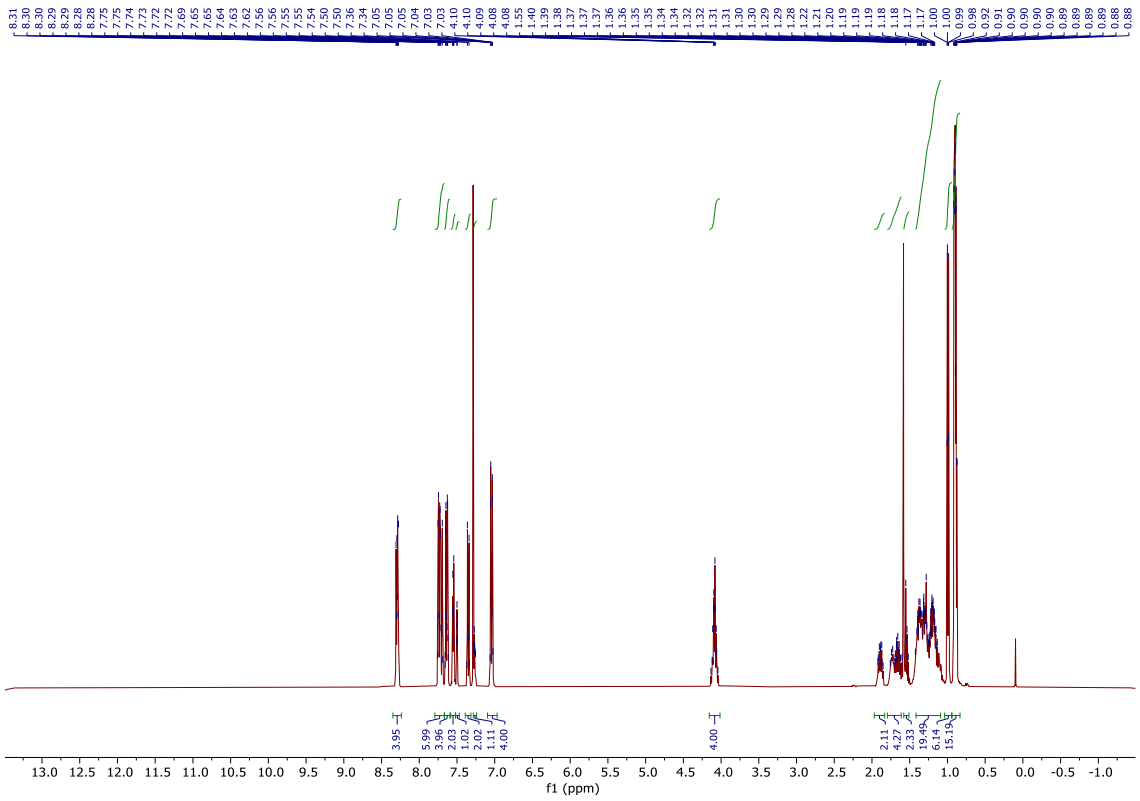
f1 (ppm)

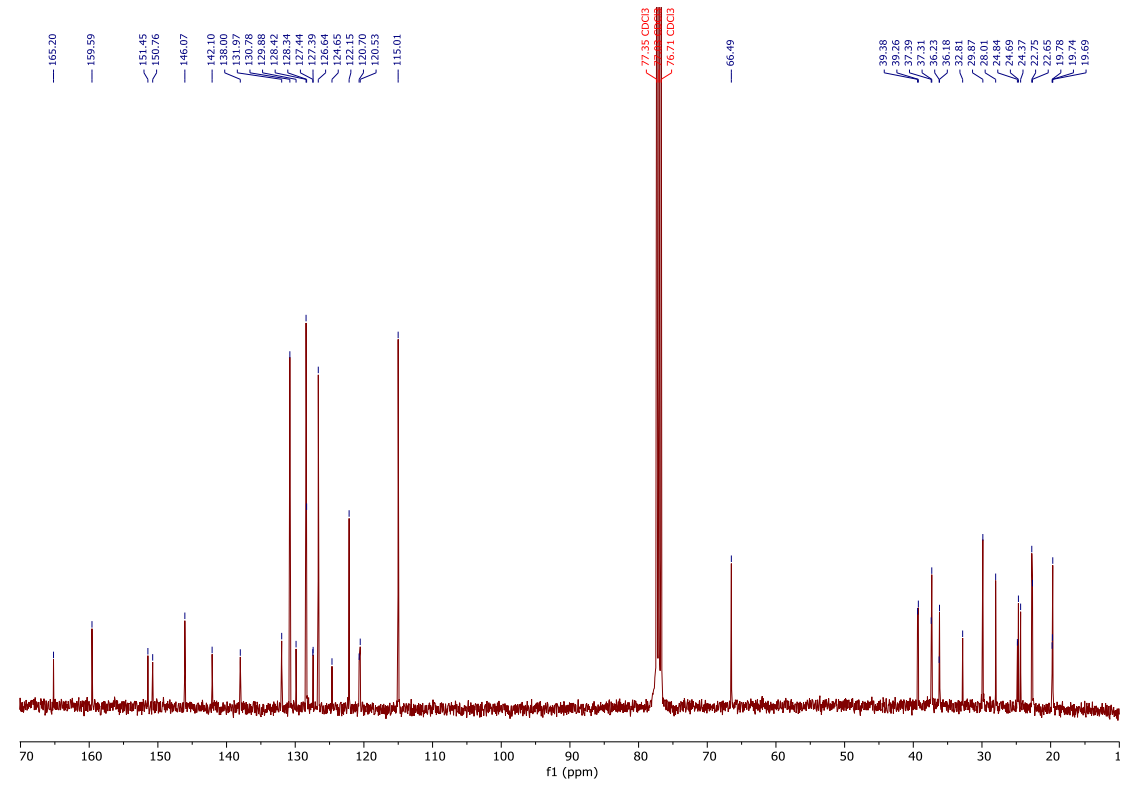
77.35 CDCl3
76.71 CDCl3
f1 (ppm)

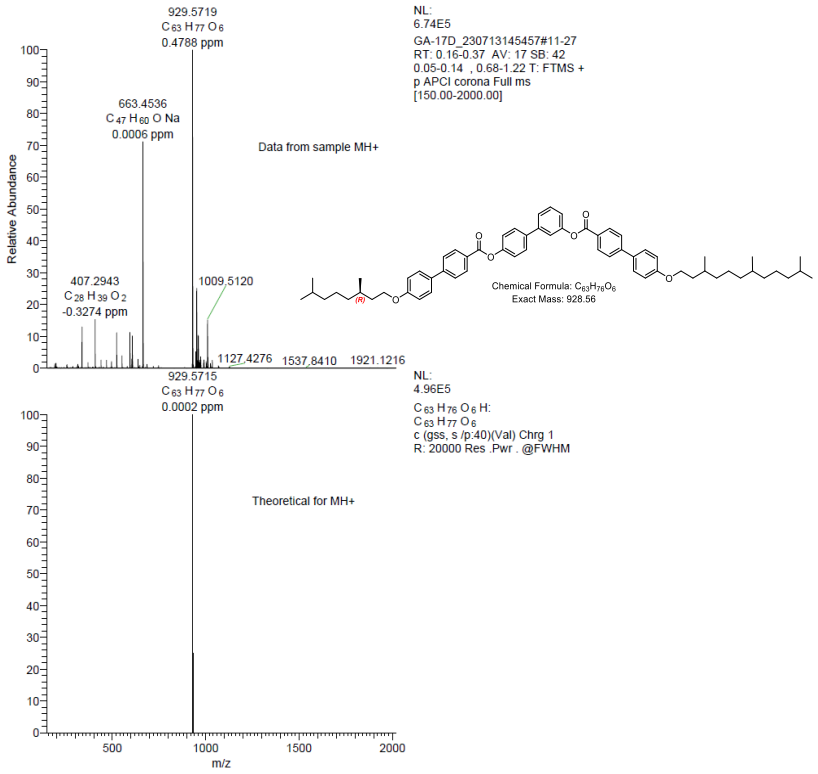

Fig. S4. ^{1}H NMR, ^{13}C NMR and HRMS spectrum of compound **BC4**.

Compound **BC5**: ^{1}H NMR ($CDCl_3$, 400 MHz, δ/ppm): δ 8.30–8.27 (m, 4H, biphenyl), 7.75–7.69 (m, 6H, biphenyl), 7.64–7.62 (m, 4H, biphenyl), 7.56–7.54 (m, 2H, biphenyl), 7.50 (m, 1H, biphenyl), 7.36–7.34 (m, 2H, biphenyl), 7.28–7.25 (m, 1H, biphenyl), 7.06–7.01 (m, 4H, biphenyl), 4.45 (h, J = 6.1 Hz, 1H, CH), 4.13–4.04 (m, 2H, CH_2), 1.92–1.85 (m, 1H), 1.82–1.61 (m, 4H), 1.58–1.48 (m, 2H), 1.43–1.28 (m, 13H), 1.22–1.17 (m, 3H), 0.99 (d, J = 6.5 Hz, 3H, CH_3), 0.93–0.90 (m, 9H, $3CH_3$). ^{13}C NMR ($CDCl_3$, 100 MHz, δ/ppm): δ 165.20 (2CO), 159.59, 158.73, 151.45, 150.74, 146.08, 142.10, 138, 131.97, 130.78, 129.87, 128.47, 128.34, 127.39, 126.63, 124.64, 122.15, 120.69, 120.53, 116.19, 115.01, 74.04, 66.49, 39.27, 37.31, 36.49, 39.18, 31.83, 29.87, 29.31, 28.01, 25.57, 24.69, 22.63, 19.78, 19.69, 14.12. HRMS. m/z: (MH^+) calcd. for ($C_{56}H_{62}O_6$): 831.4619, found: 831.4626. Spectroscopic data are shown in Fig. S5.

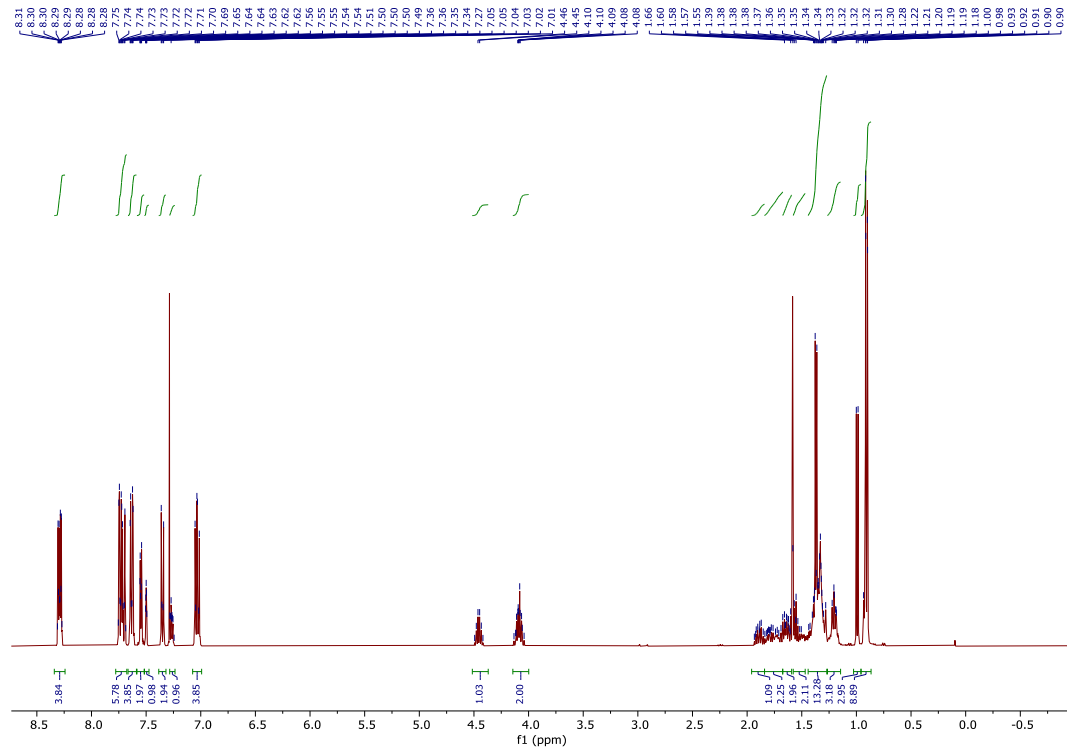
f1 (ppm)

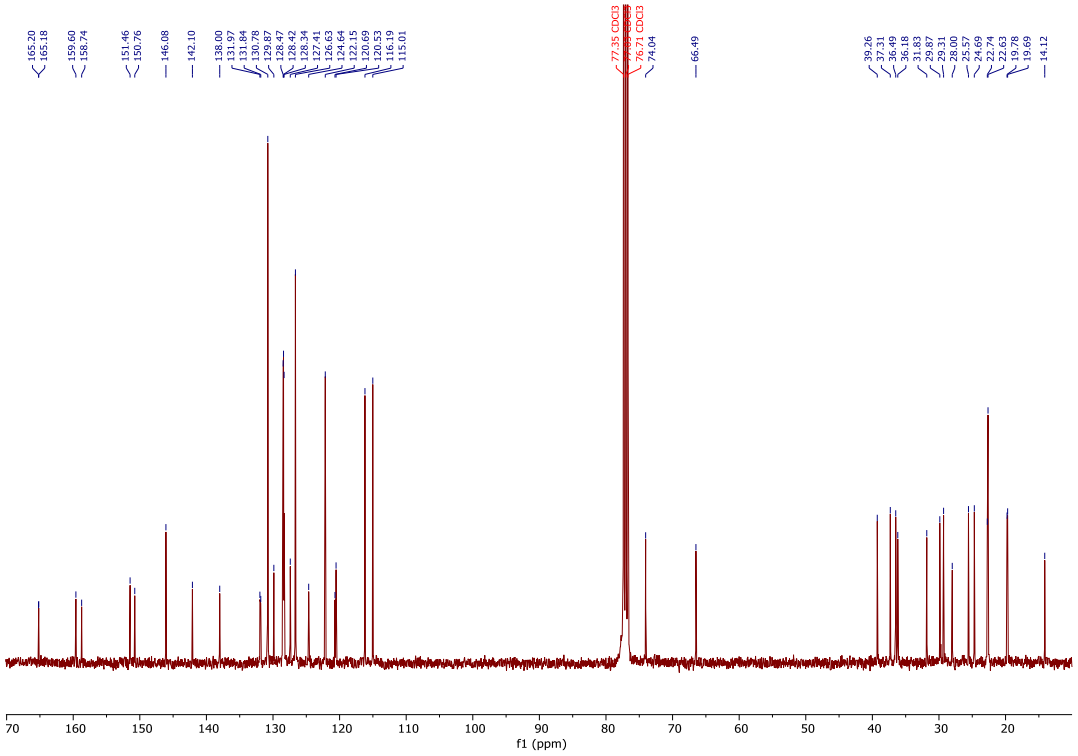
77.35 CDCl3
76.71 CDCl3
f1 (ppm)

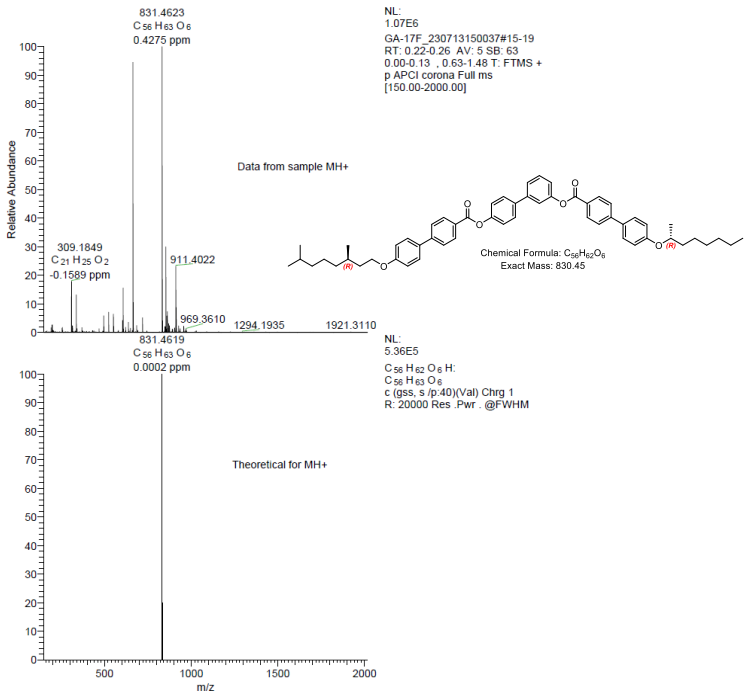

Fig. S5. ^{1}H NMR, ^{13}C NMR and HRMS spectrum of compound **BC5**.

Compound **BC6**: ^{1}H NMR ($CDCl_3$, 400 MHz, δ/ppm): δ 8.31–8.27 (m, 4H, biphenyl), 7.75–7.69 (m, 6H, biphenyl), 7.65–7.62 (m, 4H, biphenyl), 7.56–7.54 (m, 2H, biphenyl), 7.50 (dt, J = 2.3, 0.9 Hz, 1H, biphenyl), 7.36–7.34 (m, 2H, biphenyl), 7.28–7.24 (m, 1H, biphenyl), 7.05–7.01 (m, 4H, biphenyl), 4.46 (h, J = 6.1 Hz, 1H, CH), 4.13–4.04 (m, 2H, OCH_2), 1.90 (ddd, J = 12.8, 6.9, 5.0 Hz, 1H), 1.84–1.67 (m, 2H), 1.66–1.50 (m, 4H), 1.44–1.28 (m, 13H), 1.22–1.18 (m, 3H), 0.99 (d, J = 6.5 Hz, 3H, CH_3), 0.91 (dd, J = 6.6, 0.7 Hz, 9H, $3CH_3$). ^{13}C NMR ($CDCl_3$, 100 MHz, δ/ppm): δ 165.20 (2CO), 165.18, 159.60, 158.74, 151.46, 150.76, 146.08, 142.10, 138, 131.97, 131.84, 130.78, 129.87, 128.47,128.42, 128.34, 127.41, 126.63, 124.64, 122.15, 120.69, 120.53, 116.19, 115.01, 74.04, 66.49, 39.26, 37.31, 36.49, 36.18, 31.83, 29.87, 29.31, 28, 25.57, 24.69, 22.74, 22.63, 19.78, 19.69, 14.12. HRMS. m/z: (MH^+) calcd. for ($C_{56}H_{62}O_6$): 831.4619, found: 831.4623. Spectroscopic data are shown in Fig. S6.

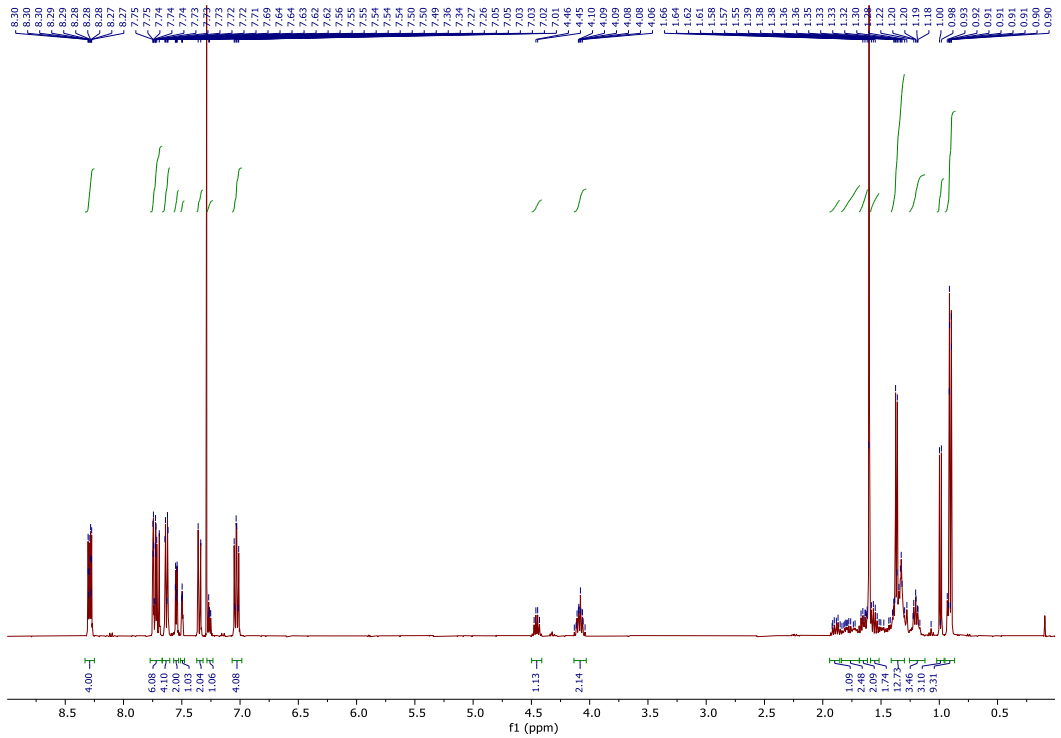
f1 (ppm)

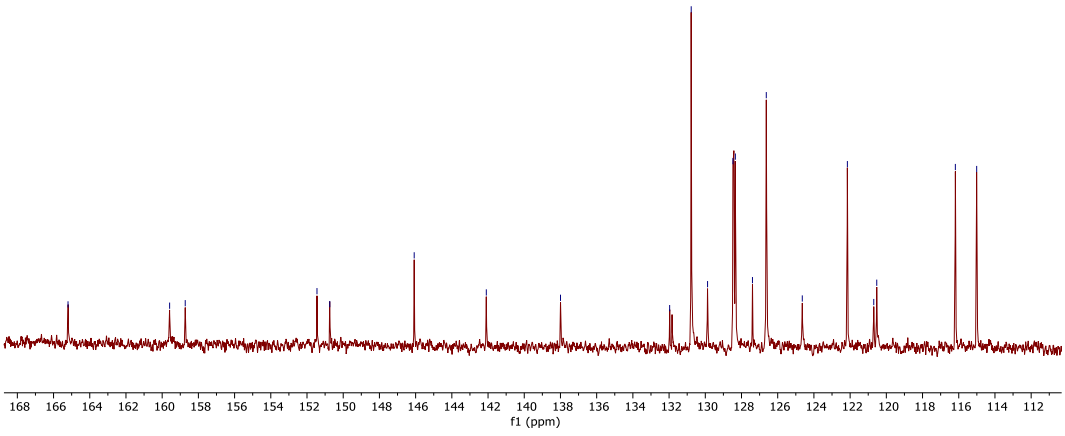
f1 (ppm)

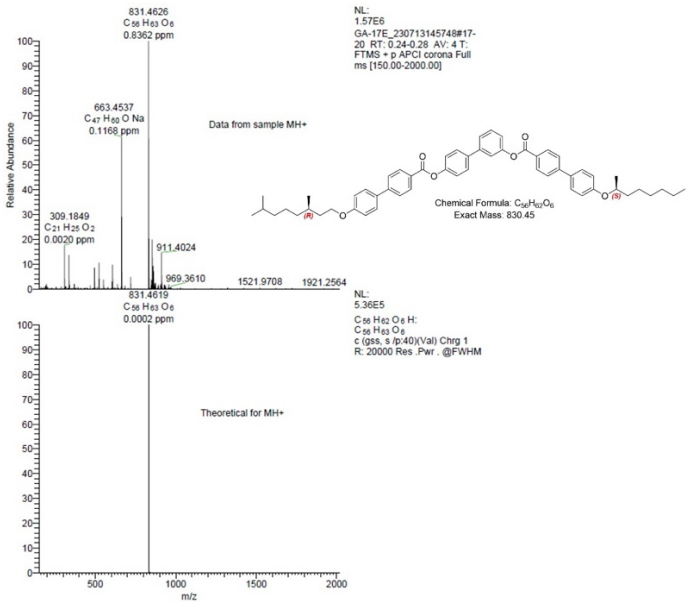

Fig. S6. ^{1}H NMR, ^{13}C NMR and HRMS spectrum for compound **BC6**.

Section S2. Differential Scanning Calorimetry (DSC) Data

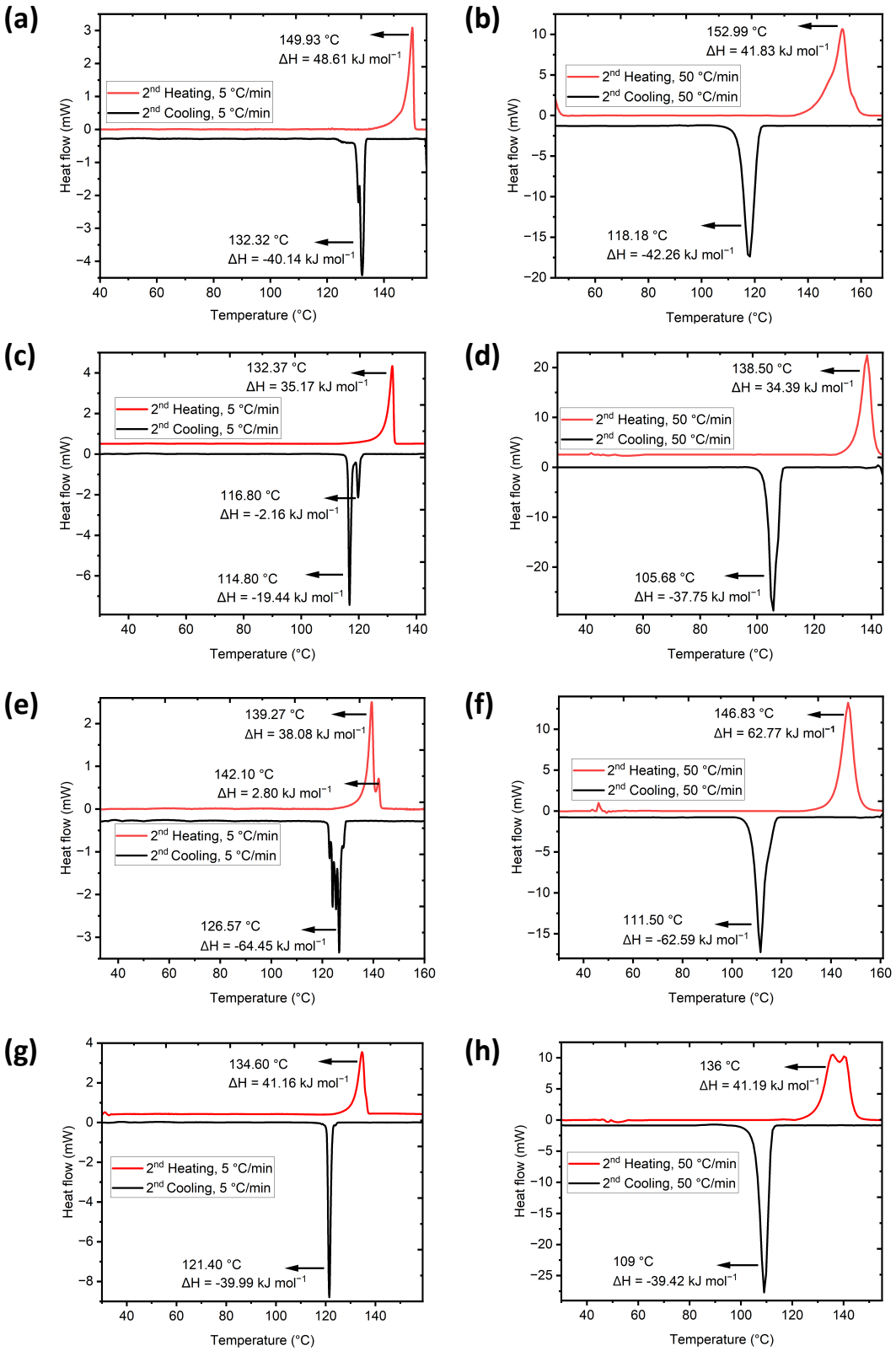

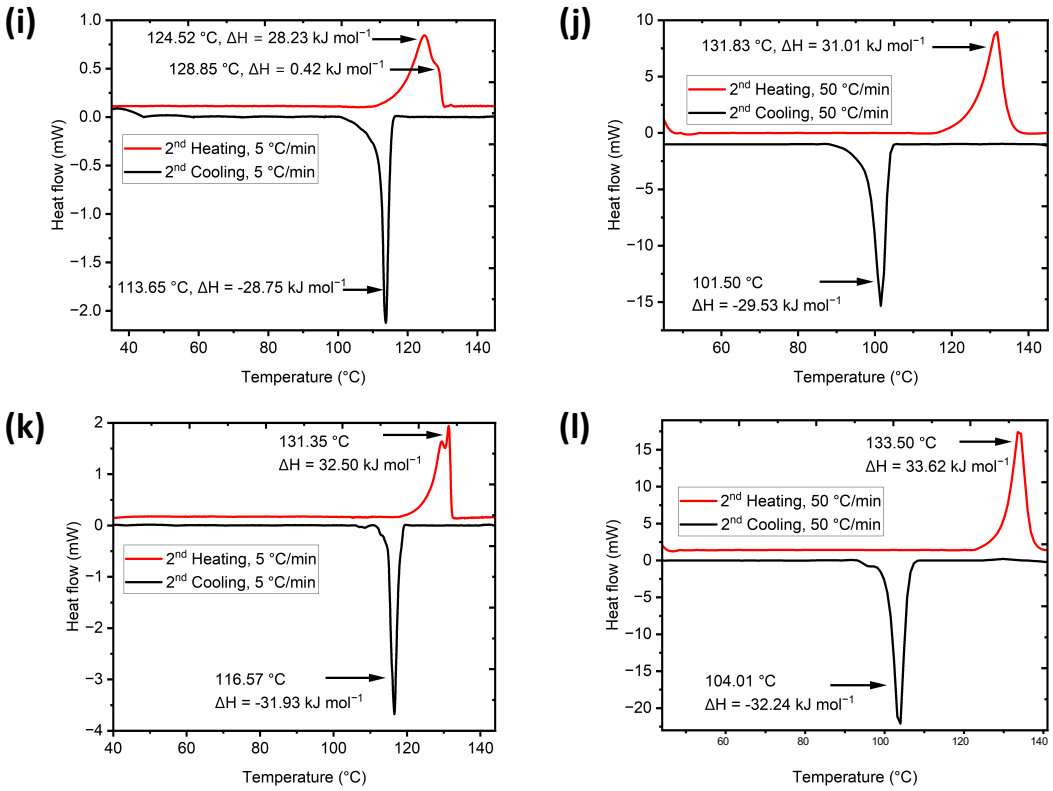

Fig. S7. DSC plots for final bent-core compounds **BC1** – **BC6** (left column: heating/cooling rate = 5 °C min^{-1}; right column: heating/cooling rate = 50 °C min^{-1}): (a, b) BC1, (c, d) BC2, (e, f) BC3, (g, h) BC4, (i, j) BC5, and (k, l) BC6.

Table S1. Phase transition temperatures (peak in DSC, °C) and enthalpy of phase transition (ΔH, kJ mol^{-1}, in [parentheses]) of bent-core molecules **BC1** – **BC6**.

#	rate / °C min^{-1}	phase transition temperature (°C) and [enthalpy] (kJ mol^{-1})	
		On heating	On cooling / °C [kJ mol^{-1}]
BC1	5	149.93 [48.61]	132.32 [–40.14]
	50	152.99 [41.83]	118.18 [–42.26]
BC2	5	132.37 [35.17]	116.80 [–2.16]; 114.80 [–19.44]
	50	138.50 [34.69]	105.68 [–37.75]
BC3	5	139.27 [38.08]; 142.10 [2.80]	126.57 [–64.45]
	50	146.83 [62.77]	111.50 [–62.59]
BC4	5	134.60 [41.16]	121.40 [–39.99]
	50	136 [41.19]	109 [–39.42]
BC5	5	124.52 [28.23]; 128.85 [0.42]	113.65 [–28.75]
	50	131.83 [31.01]	101.50 [–29.53]
BC6	5	131.35 [32.50]	116.57 [–31.93]
	50	133.50 [33.62]	104.01 [–32.24]

Section S3. Additional POM Images

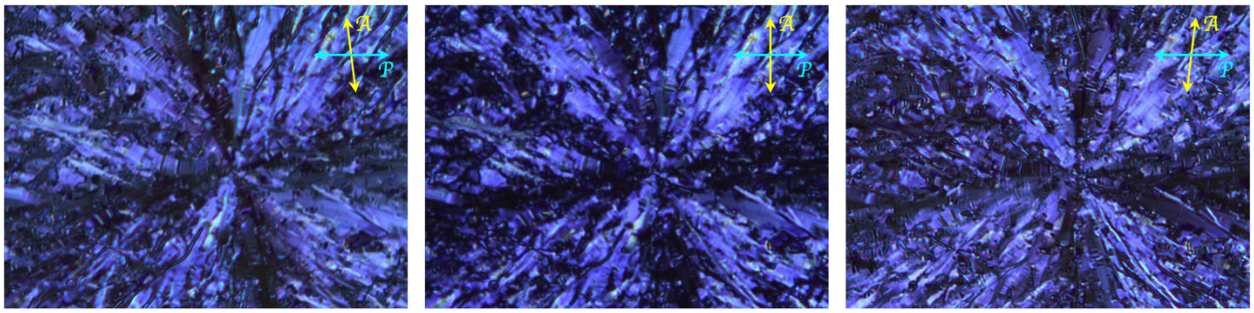

Fig. S8. Polarized optical photomicrographs of **BC2** (crossed polarizers: center image; uncrossed polarizers at left and right) after heating to the isotropic liquid phase and slow cooling at a rate of < 5 °C min^{-1} at a temperature of T = 117 °C (slight deviation of temperature calibration between DSC and Linkam heating stage as DSC shows phase transition at 116.8 °C on cooling).

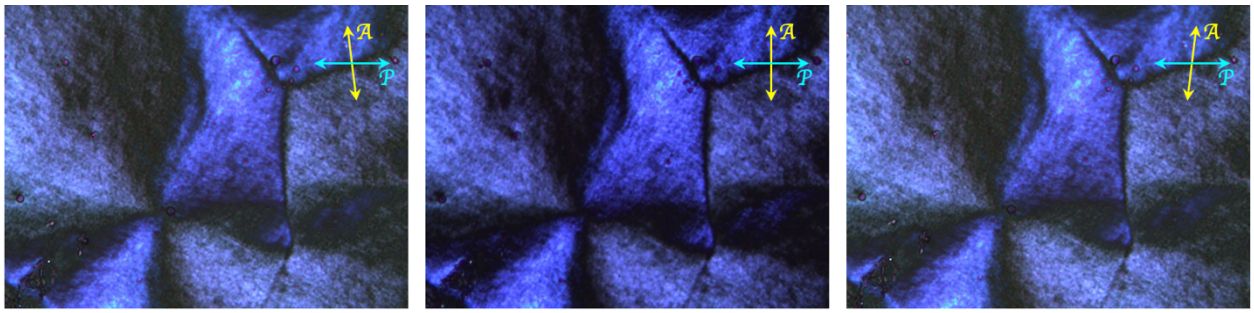

Fig. S9. Polarized optical photomicrographs of **BC6** (crossed polarizers: center image; uncrossed polarizers at left and right) after heating to the isotropic liquid phase and slow cooling to room temperature (T ~ 20 °C) at a rate of < 5 °C min^{-1}. As an example for **BC3**, **BC5**, and **BC6**, no alternating darker and brighter domains are visible upon uncrossing the polarizers in opposite directions.

Section S4. Additional SEM and TEM Images

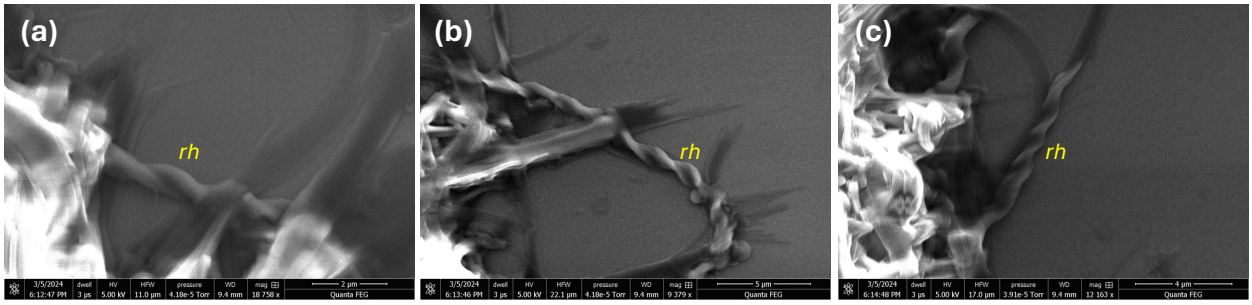

Fig. S10. (a) – (c) SEM images of **BC4** taken after slow cooling (at a rate of 5 °C min^{-1}) from the isotropic liquid state showing isolated right-handed (*rh*) HμFs.

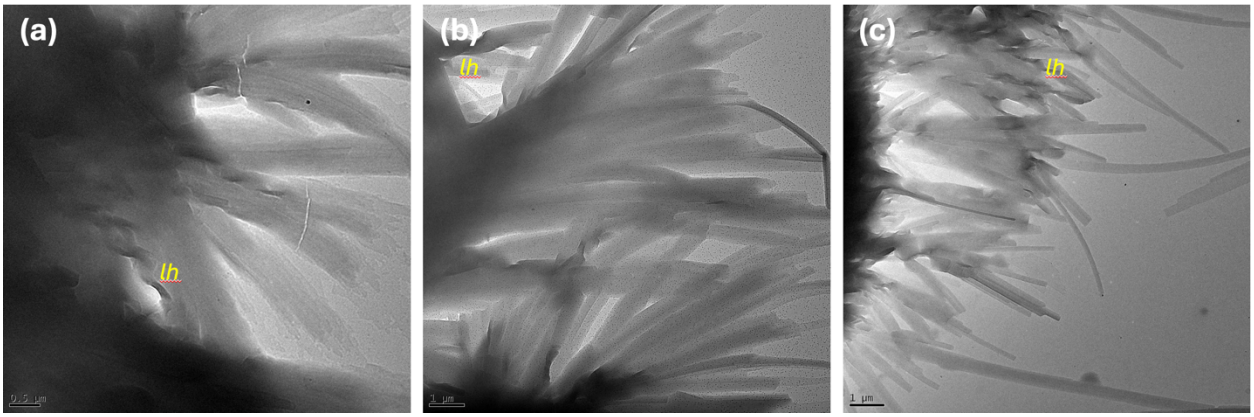

Fig. S11. (a) – (c) TEM images of **BC1** taken after slow cooling (at a rate of 5 °C min^{-1}) from the isotropic liquid state showing isolated left-handed (*lh*) HμFs.

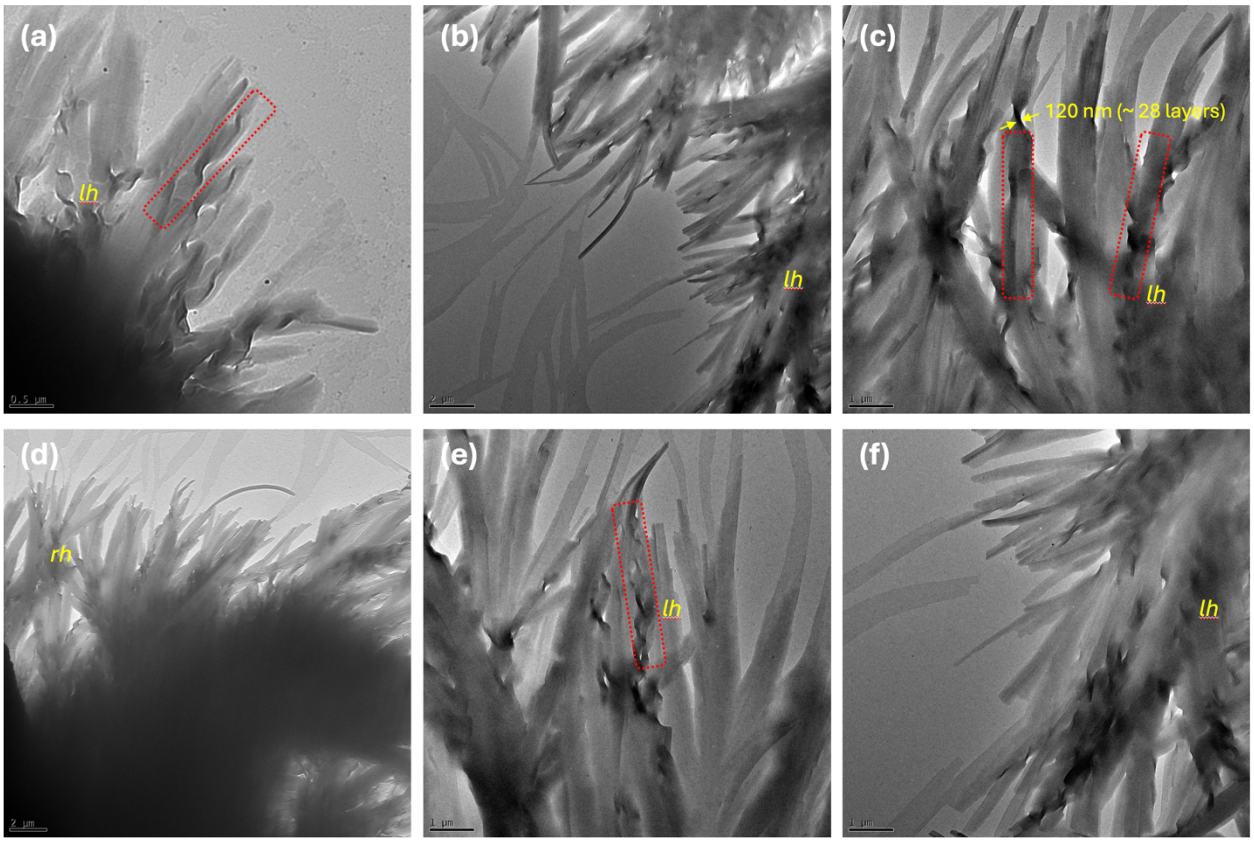

Fig. S12. (a) – (f) TEM images of **BC1** taken after rapid cooling (at a rate of ≥50 °C min^{-1}) from the isotropic liquid state showing both left- and right-handed (*lh* and *rh*) HμFs together with FNRs varying in width. A tendency of these HμFs to unwind at the ends to FNRs is visible for some (see some highlighted with red boundary). One twisting location allowed measuring the filament height (h ~ 120 nm, which, based on XRD data, gives a number of layer of $\#_{layers}$ ~ 28.

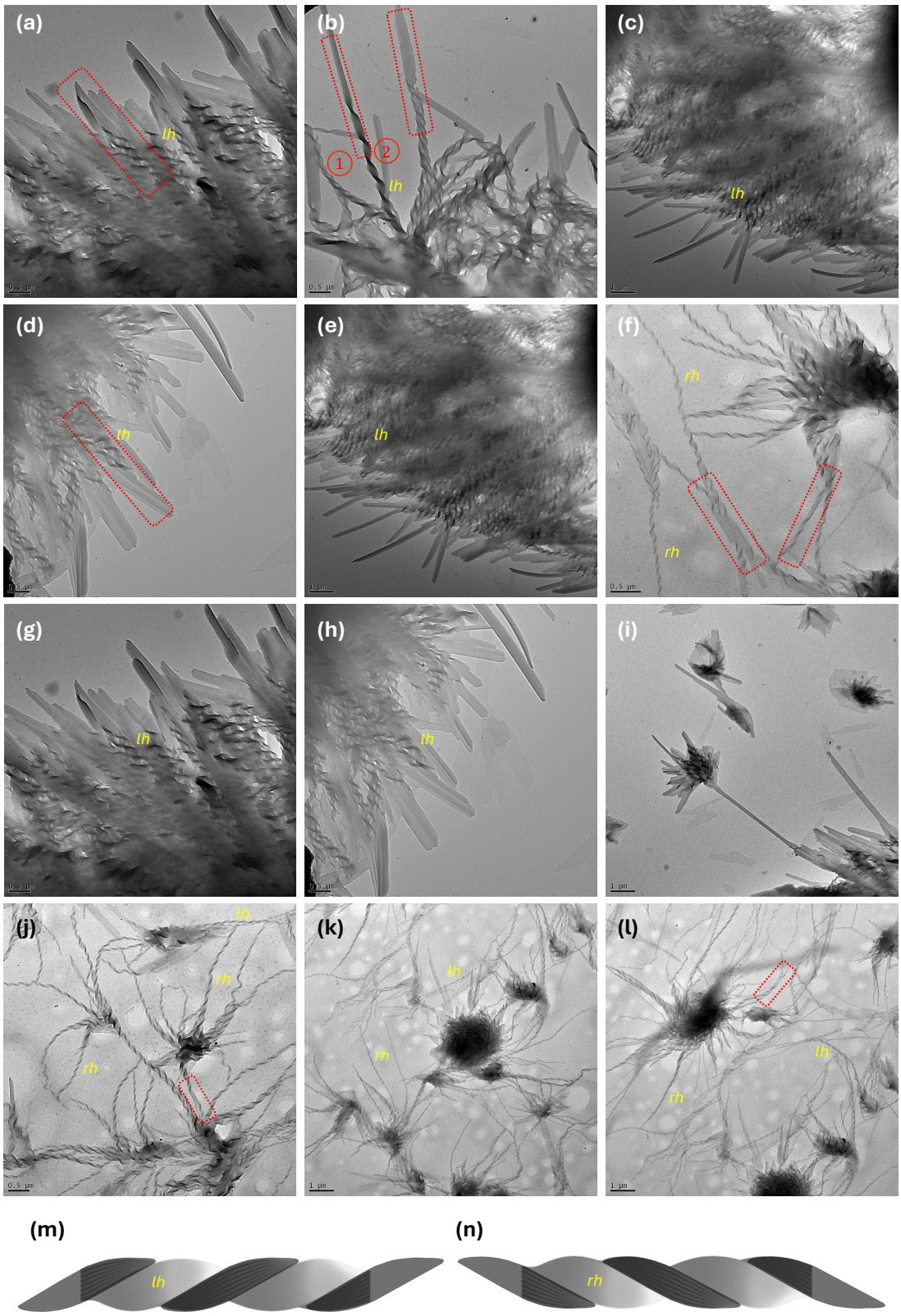

Fig. S13. (a) – (l) TEM images of **BC5** taken after slow cooling (at a rate of 5 °C min^{-1}) from the isotropic liquid state showing the coexistence of both left- and right-handed HNFs with varying

dimensions (among many examples in these images, ① in (b) indicates an HNF_a with smaller dimensions; ② in (b) a larger HNF_b with larger dimensions. (m) and (n) Models highlighting how the handedness is determined in these TEM images. Some prominent locations where transitions between HNFs and FNRs are highlighted with red boundaries.

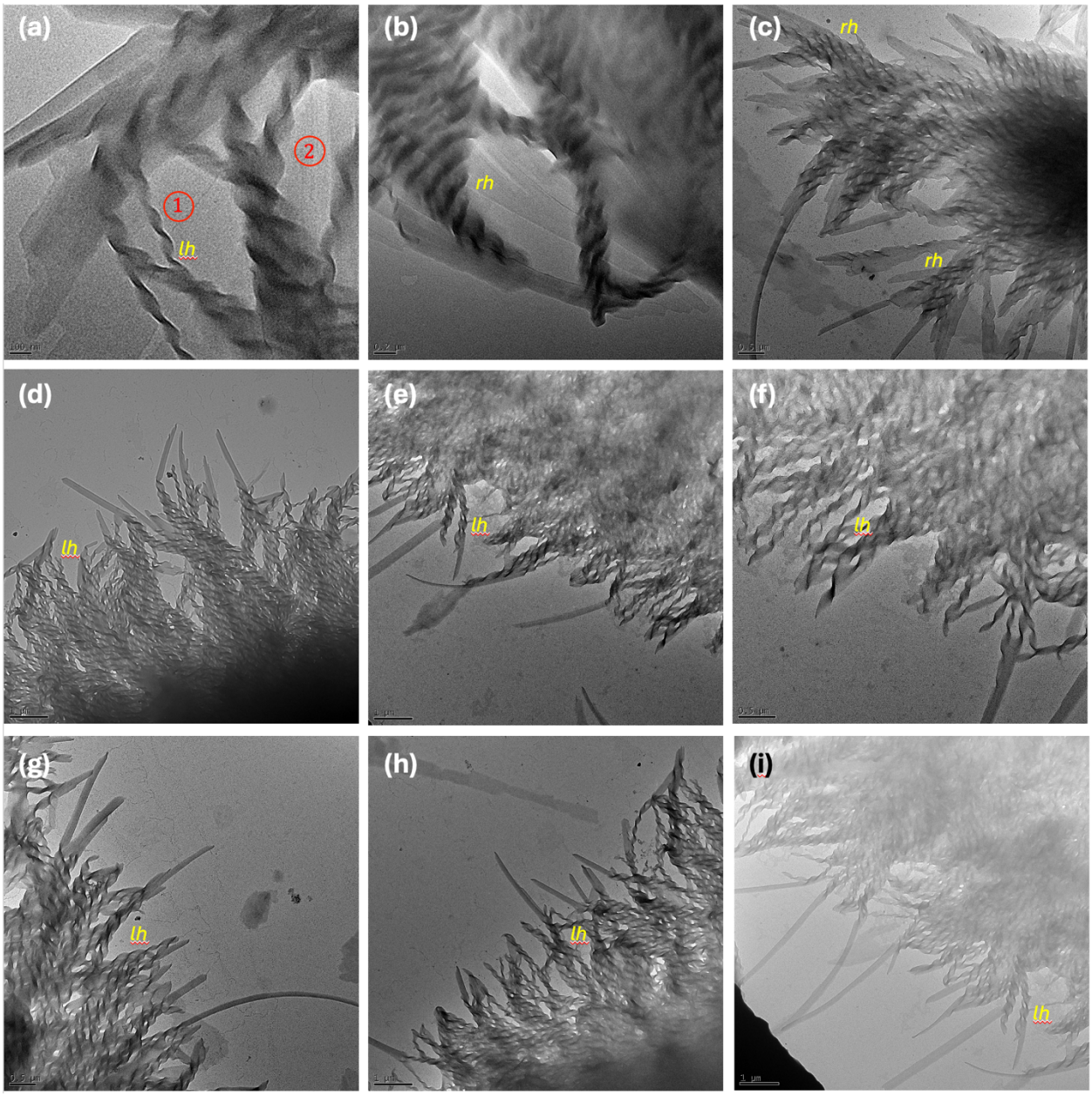

Fig. S14. (a) – (i) TEM images of **BC5** taken after rapid cooling (at a rate of ≥50 °C min^{-1}) from the isotropic liquid state showing the coexistence of both left- and right-handed HNFs varying in dimensions (① in (a) indicates an HNF_a with smaller dimensions; ② in (a) a larger HNF_b with larger dimensions.

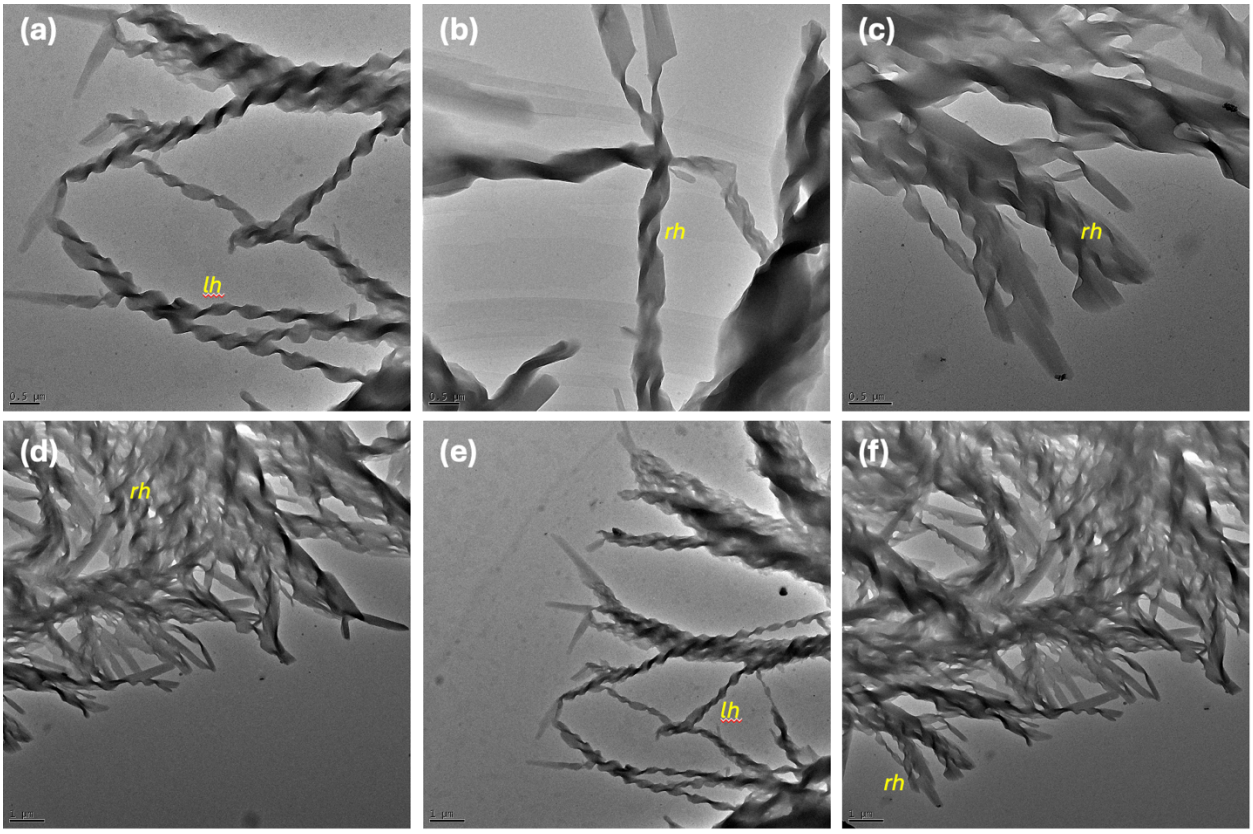

Fig. S15. (a) – (f) TEM images of **BC6** taken after slow cooling (at a rate of 5 °C min^{-1}) from the isotropic liquid state showing the coexistence of both left- and right-handed HμFs.

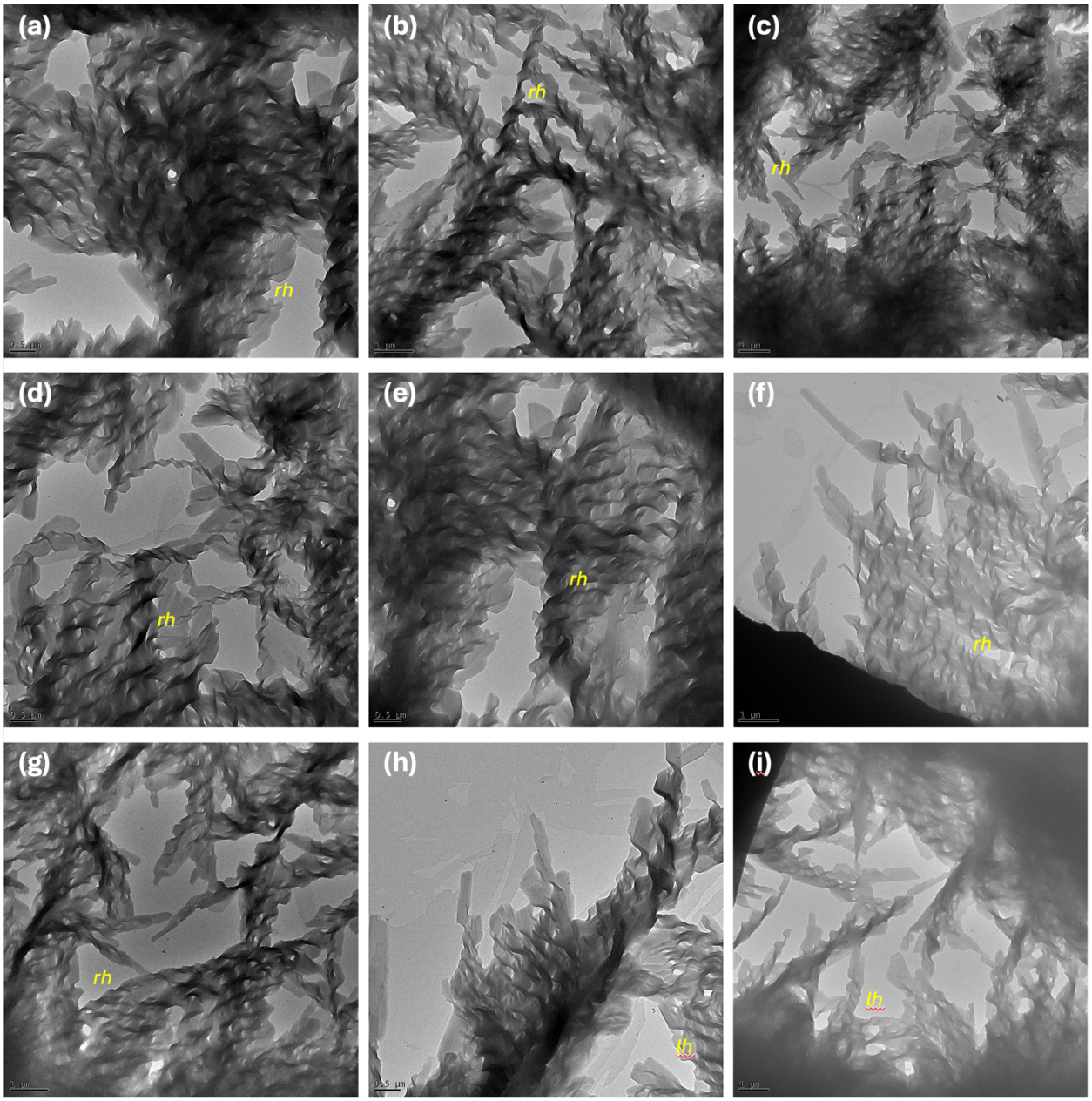

Fig. S16. (a) – (i) TEM images of **BC6** taken after rapid cooling (at a rate of ≥50 °C min^{-1}) from the isotropic liquid state showing the coexistence of both left- and right-handed HμFs.

Section S5. Additional XRD Details and Data

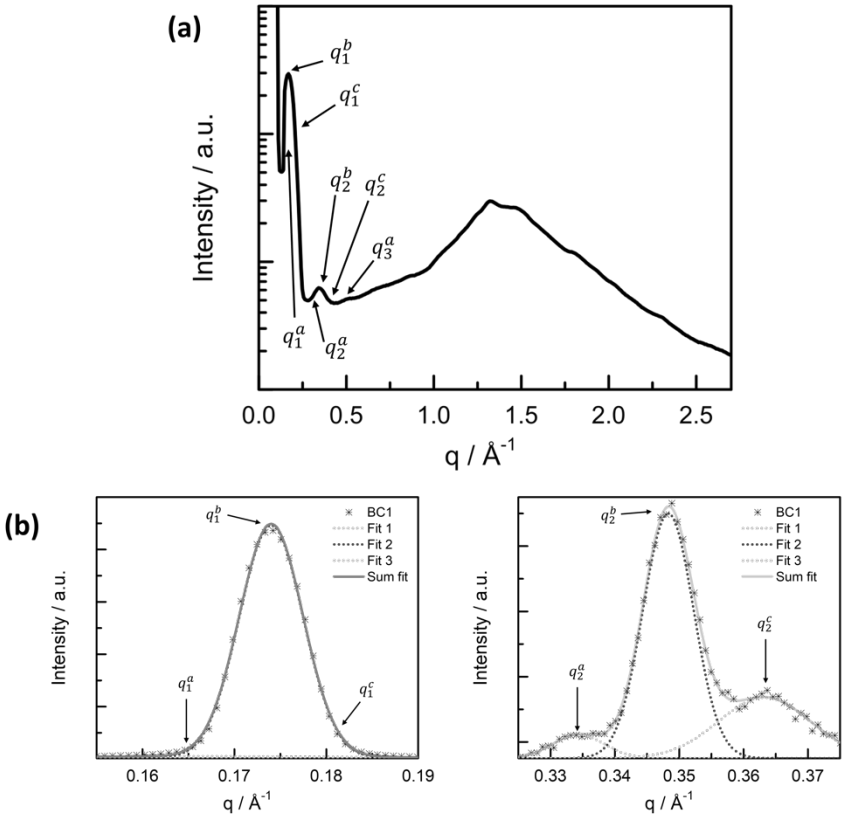

Fig. S17. (a) XRD analysis data showing intensity (a.u.) vs. wave vector q (Å^{-1}) of the combined MAXD-WAXD region for **BC1** taken after slow cooling from the isotropic liquid phase at room temperature. (b) Peak deconvolutions; for peak positions, relative intensity values, and Miller indices, see Table S2.

Table S2. Peak positions, assignment, relative intensity values, and Miller indices for the three B4 structures formed by **BC1** upon slow cooling.

q/Å^{-1}	*Assignment*	*Relative Intensity*	*Index*		
			B4 Phase 1	*B4 Phase 2*	*B4 Phase 3*
0.165	q_1^a	3.90×10^8	001		
0174	q_1^b	2.09×10^{10}		001	
0.181	q_1^c	1.84×10^9			001
0.334	q_2^a	6.12×10^6	002		
0.348	q_2^b	1.03×10^7		002	
0.363	q_2^c	7.71×10^6			002
0.501	q_3^a	1.12×10^8	003		

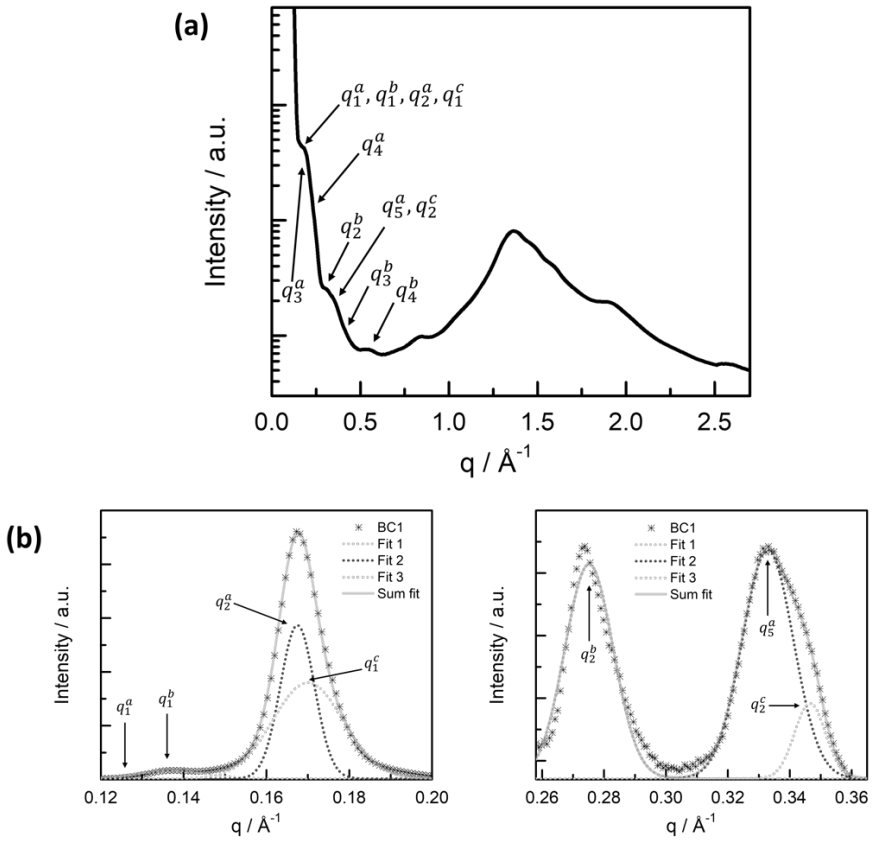

Fig. S18. (a) XRD analysis data showing intensity (a.u.) vs. wave vector q (Å^{-1}) of the combined MAXD-WAXD region for **BC1** taken after rapid cooling from the isotropic liquid phase at room temperature. (b) Peak deconvolutions; for peak positions, relative intensity values, and Miller indices, see Table S3.

Table S3. Peak positions, assignment, relative intensity values, and Miller indices for the three B4 structures formed by **BC1** upon rapid cooling.

q/Å^{-1}	Assignment	Relative Intensity	Index		
			B4 Phase 1	B4 Phase 2	B4 Phase 3
0.124	q_1^a	6.50×10^7	100		
0.137	q_1^b	2.13×10^8		001	
0.167	q_2^a	4.28×10^9	001		
0.169	q_1^c	4.19×10^9			001
0.208	q_3^a	9.13×10^7	101		
0.245	q_4^a	4.60×10^7	200		
0.275	q_2^b	6.29×10^7		002	
0.333	q_5^a	5.87×10^7	002		
0.340	q_2^c	2.06×10^7			002
0.408	q_3^b	1.84×10^7		003	
0.539	q_4^b	1.60×10^7		004	

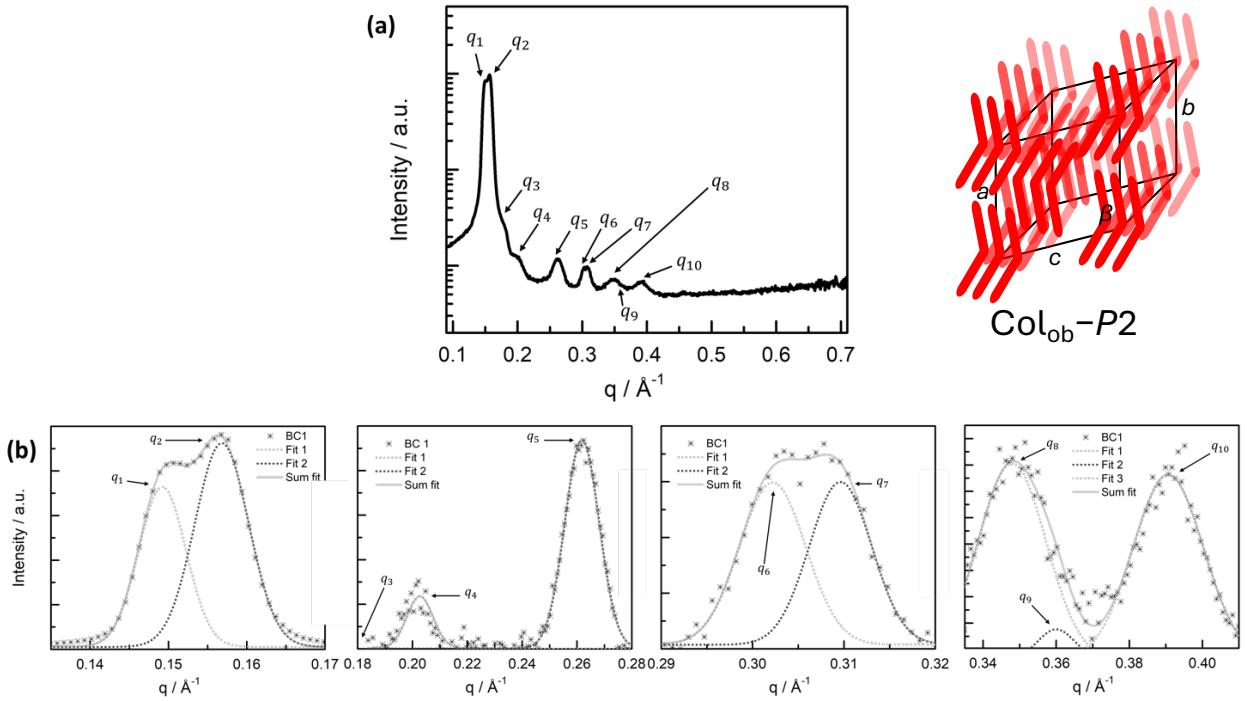

Fig. S19. (a) XRD analysis data showing intensity (a.u.) vs. wave vector q (Å^{-1}) of the MAXD-region for **BC1** taken after rapid cooling from the isotropic liquid phase at room temperature at a different sample location. (b) Peak deconvolutions; for peak positions, relative intensity values, and Miller indices, see Table S4.

Table S4. Peak positions, assignment, relative intensity values, and Miller indices for B1 (Col_{ob}−*P*2) structures formed by **BC1** upon rapid cooling (different sample location).

q/Å^{-1}	*Assignment*	*Relative Intensity*	*Index: Col_{ob}−P2*
0.149	q_1	8.19×10^9	001
0.157	q_2	9.62×10^9	100
0.180	q_3	2.36×10^7	010
0.203	q_4	1.21×10^7	101
0.262	q_5	1.12×10^7	111
0.302	q_6	9.43×10^6	002
0.310	q_7	9.70×10^6	200
0.349	q_8	7.11×10^6	$11\bar{2}$
0.360	q_9	5.19×10^6	020
0.391	q_{10}	6.89×10^7	120

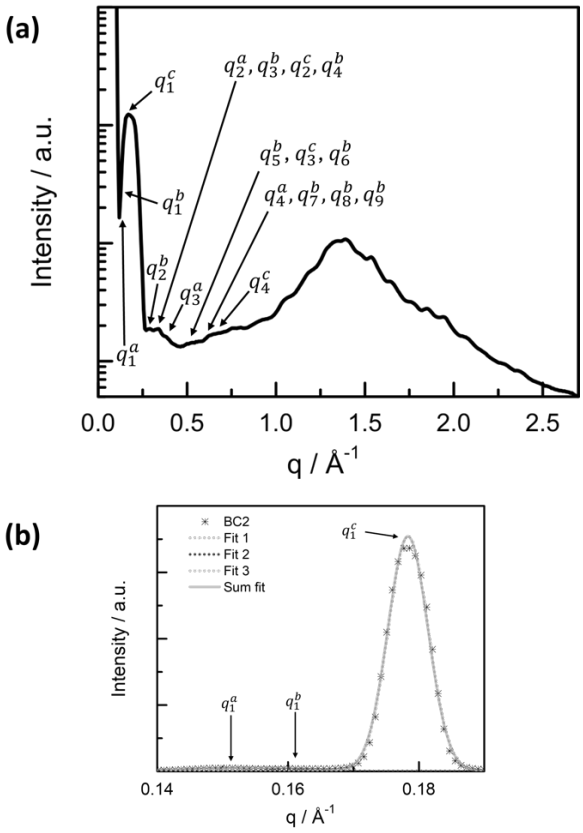

Fig. S20. (a) XRD analysis data showing intensity (a.u.) vs. wave vector q (Å^{-1}) of the combined MAXD-WAXS region for **BC2** taken after slow cooling from the isotropic liquid phase at room temperature. (b) Peak deconvolution; for data see Table S5.

Table S5. Peak positions, assignment, relative intensity values, and Miller indices for two B4 and the B1 Col$_r$–*c2mm* structures formed by **BC2** upon slow cooling.

q/Å^{-1}	*Assignment*	*Relative Intensity*	*Index*		
			B4 Phase 1	*B4 Phase 2*	*Col$_r$*
0.151	q_1^a	1.07×10^8	001		
0.161	q_1^b	8.99×10^7			001
0.178	q_1^c	6.63×10^{19}		001	
0.257	q_2^b	1.03×10^7			101
0.302	q_2^a	3.12×10^7	002		
0.318	q_3^b	9.33×10^6			002
0.357	q_2^c	1.85×10^7		002	
0.381	q_4^b	1.42×10^7			102
0.453	q_3^a	1.23×10^7	003		
0.524	q_5^b	1.04×10^7			103
0.535	q_3^c	1.13×10^7		003	
0.59	q_6^b	9.21×10^6			301
0.604	q_4^a	1.03×10^6	004		
0.630	q_7^b	1.62×10^7			203
0.665	q_8^b	1.19×10^7			104
0.69	q_9^b	1.34×10^7			302
0.713	q_4^c	1.33×10^7		004	

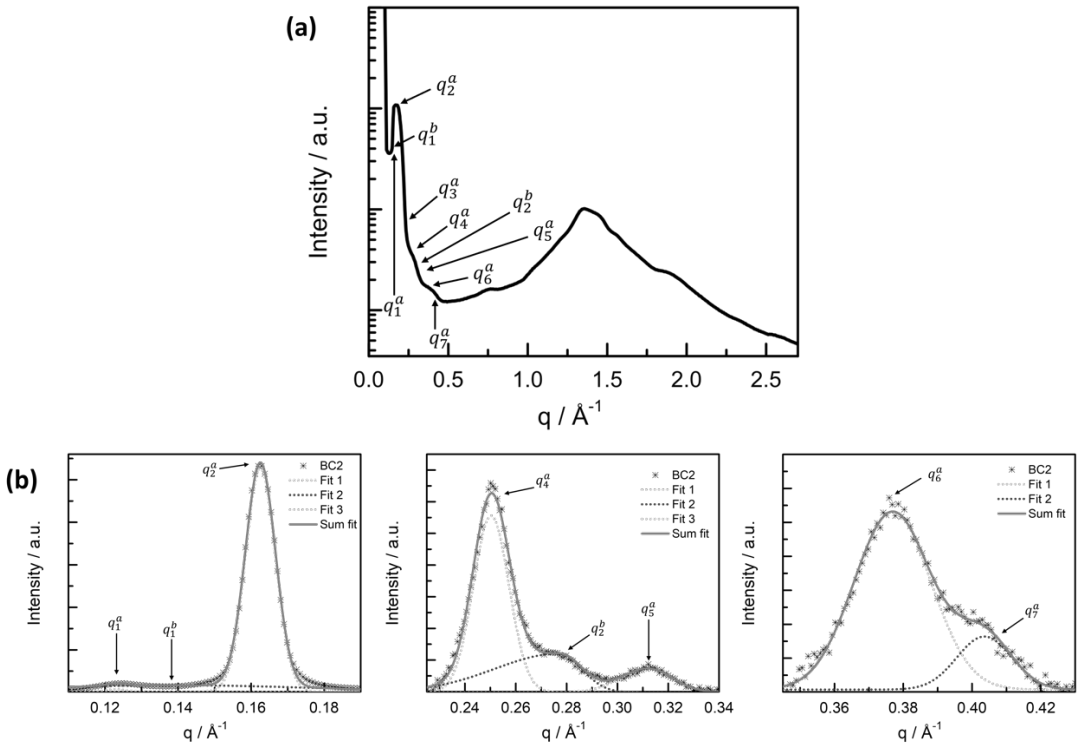

Fig. S21. (a) XRD analysis data showing intensity (a.u.) vs. wave vector q (Å^{-1}) of the combined MAXD-WAXS region for **BC2** taken after rapid cooling from the isotropic liquid phase at room temperature. (b) Peak deconvolution; for data see Table S6.

Table S6. Peak positions, assignment, relative intensity values, and Miller indices for the B4 structures formed by **BC2** upon rapid cooling.

q/Å^{-1}	*Assignment*	*Relative Intensity*	*Index*	
			B4 Phase 1	*B4 Phase 2*
0.123	q_1^a	1.06×10^9	100	
0.139	q_1^b	7.40×10^8		001
0.161	q_2^a	2.66×10^{10}	001	
0.202	q_3^a	2.88×10^8	101	
0.249	q_4^a	2.43×10^8	200	
0.278	q_2^b	1.12×10^8		002
0.312	q_5^a	8.48×10^7	002	
0.375	q_6^a	7.85×10^7	300	
0.403	q_7^a	5.93×10^7	202	

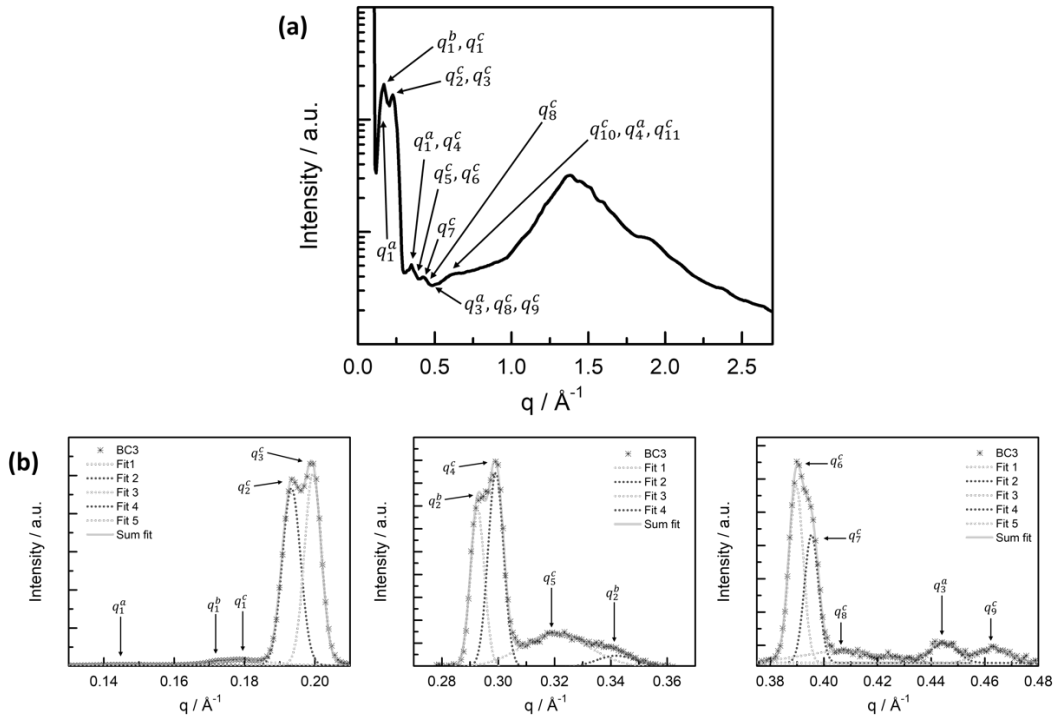

Fig. S22. (a) XRD analysis data showing intensity (a.u.) vs. wave vector q (Å^{-1}) of the combined MAXD-WAXS region for **BC3** taken after slow cooling from the isotropic liquid phase at room temperature. (b) Peak deconvolution; for data see Table S7.

Table S7. Peak positions, assignment, relative intensity values, and Miller indices for two B4 structures and the coexisting Col_{ob} phase formed by **BC3** upon slow cooling.

q/Å^{-1}	*Assignment*	*Relative Intensity*	*Index*		
			B4 Phase 1	*B4 Phase 2*	*Col_{ob}*
0.145	q_1^a	3.26×10^7	001		
0.172	q_1^b	7.48×10^7		001	
0.179	q_1^c	8.99×10^7			001
0.193	q_2^c	2.51×10^9			100
0.199	q_3^c	2.83×10^9			010
0.293	q_2^a	2.02×10^7	002		
0.299	q_4^c	2.34×10^7			110
0.320	q_5^c	7.96×10^6			111
0.342	q_2^b	6.97×10^6		002	
0.389	q_6^c	1.72×10^7			002
0.395	q_7^c	1.96×10^7			102
0.406	q_8^c	1.46×10^7			020
0.440	q_3^a	6.38×10^6	003		
0.463	q_9^c	6.36×10^6			211
0.557	q_{10}^c	7.51×10^6			103
0.584	q_4^a	9.01×10^6	004		
0.621	q_{11}^c	8.30×10^6			310

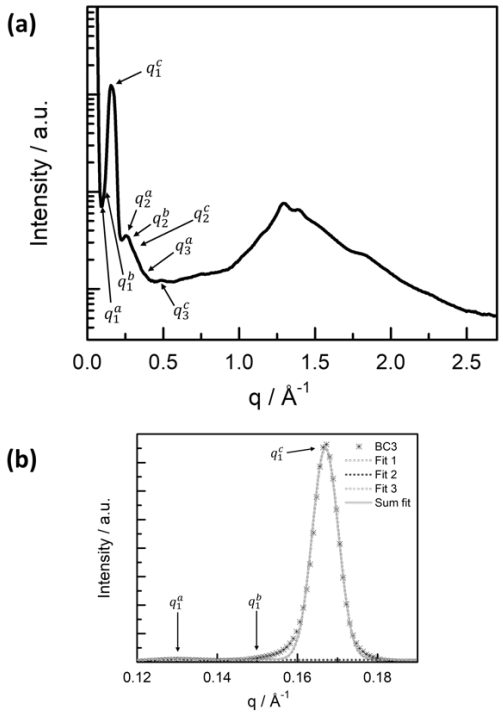

Fig. S23. (a) XRD analysis data showing intensity (a.u.) vs. wave vector q (Å^{-1}) of the combined MAXD-WAXS region for **BC3** taken after rapid cooling from the isotropic liquid phase at room temperature. (b) Peak deconvolution; for data see Table S6.

Table S8. Peak positions, assignment, relative intensity values, and Miller indices for B4 structures formed by **BC3** upon rapid cooling.

q/Å^{-1}	*Assignment*	*Relative Intensity*	*Index*		
			B4 Phase 1	*B4 Phase 2*	*B4 Phase 3*
0.129	q_1^a	1.90×10^8	001		
0.151	q_1^b	3.21×10^8		001	
0.167	q_1^c	7.58×10^9			001
0.260	q_2^a	5.65×10^7	002		
0.295	q_2^b	3.72×10^7		002	
0.334	q_2^c	3.39×10^7			002
0.387	q_3^a	1.99×10^7	003		
0.495	q_3^a	1.23×10^7			003

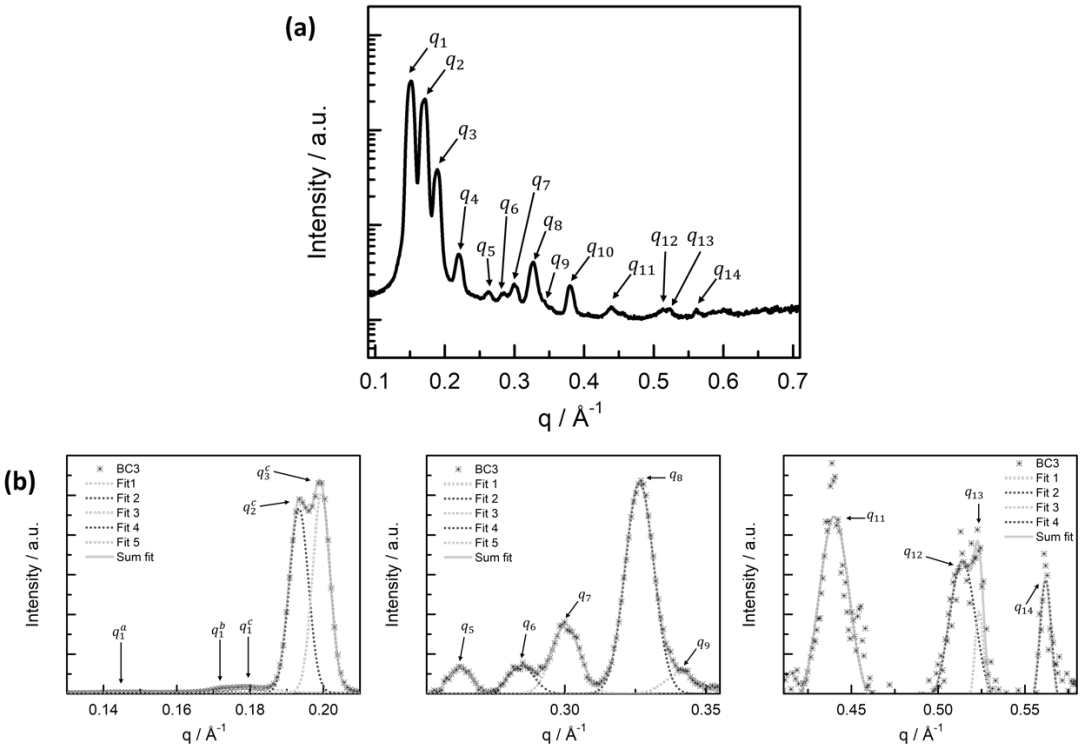

Fig. S24. (a) XRD analysis data showing intensity (a.u.) vs. wave vector q (Å^{-1}) of the MAXD-region for **BC3** on 2nd heating at T = 140 °C. (b) Peak deconvolution; for data see Table S9.

Table S9. Peak positions, assignment, relative intensity values, and Miller indices for the B1 (Col_{ob}–$P2$) phase formed by **BC3** on second heating at T = 140 °C.

q/Å^{-1}	*Assignment*	*Relative Intensity*	*Index*
0.151	q_1	3.26×10^9	001
0.170	q_2	2.06×10^9	100
0.189	q_3	3.61×10^8	010
0.221	q_4	4.82×10^7	101
0.263	q_5	1.94×10^7	110
0.285	q_6	1.87×10^7	111
0.300	q_7	2.38×10^7	002
0.327	q_8	4.05×10^7	102
0.341	q_9	1.56×10^7	200
0.379	q_{10}	2.28×10^7	020
0.440	q_{11}	1.35×10^7	202
0.514	q_{12}	1.31×10^7	300
0.524	q_{13}	1.13×10^7	311
0.562	q_{14}	1.28×10^7	030

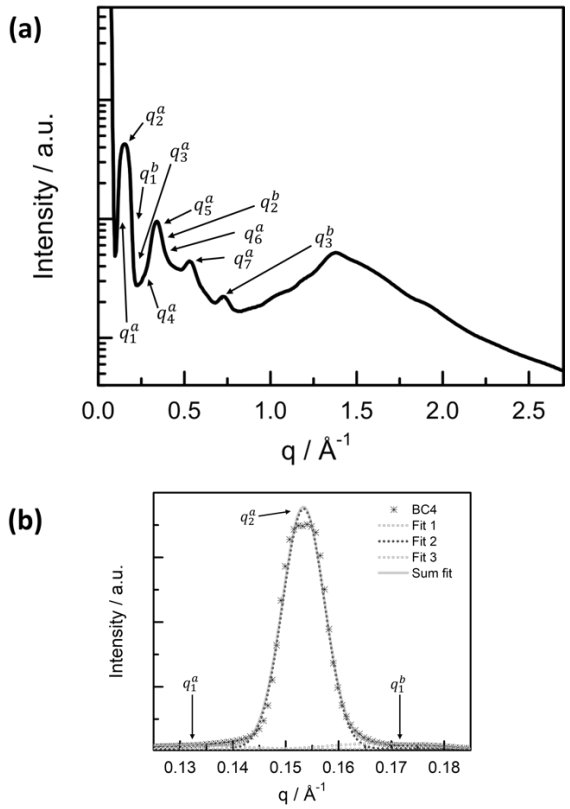

Fig. S25. (a) XRD analysis data showing intensity (a.u.) vs. wave vector q (Å^{-1}) of the combined MAXD-WAXS region for **BC4** taken after slow cooling from the isotropic liquid phase at room temperature. (b) Peak deconvolution; for data see Table S10.

Table S10. Peak positions, assignment, relative intensity values, and Miller indices for the two B4 structures formed by **BC4** upon slow cooling.

q/Å^{-1}	*Assignment*	*Relative Intensity*	*Index*	
			B4 Phase 1	*B4 Phase 2*
0.130	q_1^a	8.79×10^7	100	
0.153	q_2^a	3.49×10^9	001	
0.172	q_1^b	9.16×10^7		001
0.200	q_3^a	3.50×10^7	101	
0.261	q_4^a	3.68×10^7	200	
0.31	q_5^a	2.82×10^7	002	
0.345	q_2^b	1.97×10^7		002
0.391	q_6^a	1.80×10^7	300	
0.452	q_7^a	6.21×10^5	003	
0.523	q_8^a	4.42×10^5	400	
0.705	q_3^b	2.22×10^5		004

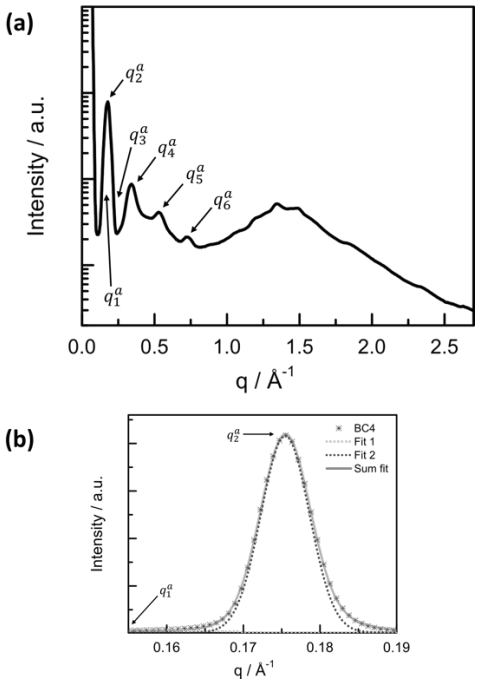

Fig. S26. (a) XRD analysis data showing intensity (a.u.) vs. wave vector q (Å^{-1}) of the combined MAXD-WAXS region for **BC4** taken after rapid cooling from the isotropic liquid phase at room temperature. (b) Peak deconvolution; for data see Table S11.

Table S11. Peak positions, assignment, relative intensity values, and Miller indices for the modulated B4 structure formed by **BC4** rapid slow cooling.

q/Å^{-1}	*Assignment*	*Relative Intensity*	*Index B4 Phase 1*
0.155	q_1^a	6.45×10^7	100
0.176	q_2^a	4.06×10^9	001
0.234	q_3^a	1.28×10^7	101
0.352	q_4^a	8.54 ×10^5	002
0.528	q_5^a	4.12×10^5	003
0.71	q_6^a	2.11×10^5	004

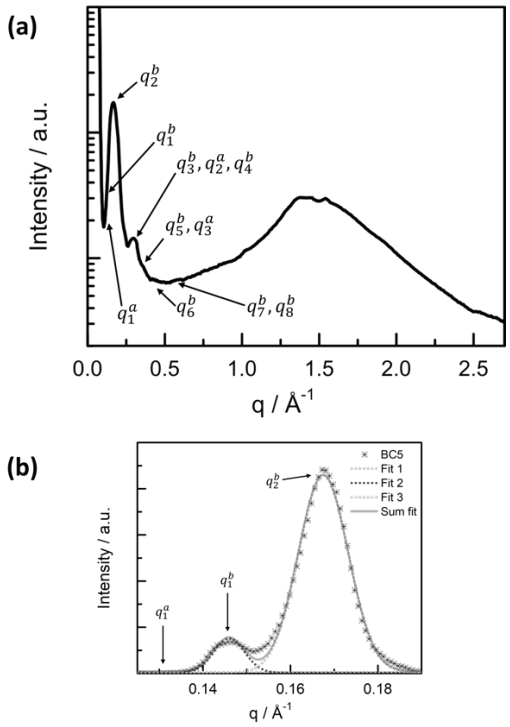

Fig. S27. (a) XRD analysis data showing intensity (a.u.) vs. wave vector q (Å^{-1}) of the combined MAXD-WAXS region for **BC5** taken after slow cooling from the isotropic liquid phase at room temperature. (b) Peak deconvolution; for data see Table S12.

Table S12. Peak positions, assignment, relative intensity values, and Miller indices for the two B4 structures formed by **BC5** upon slow cooling.

q/Å^{-1}	*Assignment*	*Relative Intensity*	*Index*	
			B4 Phase 1	*B4 Phase 2*
0.134	q_1^a	3.27×10^7	001	
0.145	q_1^b	1.69×10^8		100
0.166	q_2^b	9.12×10^8		001
0.217	q_3^b	6.04×10^7		101
0.259	q_2^a	2.29×10^7	002	
0.289	q_4^b	5.79×10^7		200
0.33	q_5^b	2.16×10^7		002
0.387	q_3^a	1.57×10^7	003	
0.436	q_6^b	1.50×10^7		300
0.503	q_7^b	1.45×10^7		004
0.570	q_8^b	1.65×10^7		400

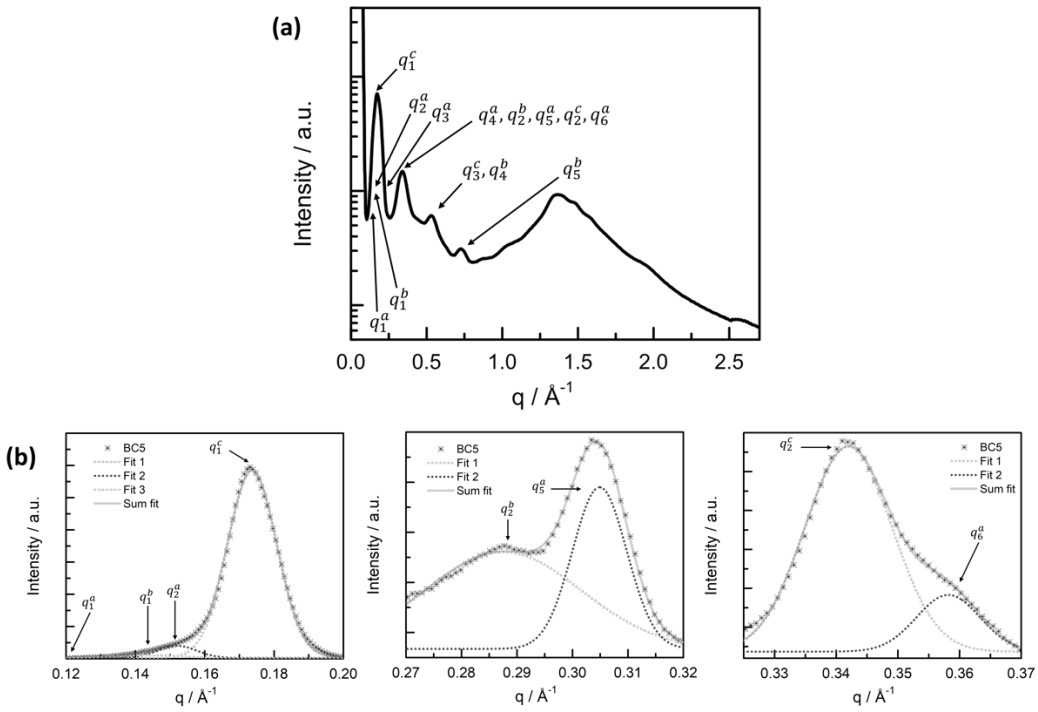

Fig. S28. (a) XRD analysis data showing intensity (a.u.) vs. wave vector q ($Å^{-1}$) of the combined MAXD-WAXS region for **BC5** taken after rapid cooling from the isotropic liquid phase at room temperature. (b) Peak deconvolution; for data see Table S12.

Table S13. Peak positions, assignment, relative intensity values, and Miller indices for the four B4 structures formed by **BC5** upon rapid cooling.

$q/Å^{-1}$	*Assignment*	*Relative Intensity*	*Index*		
			B4 Phase 1	*B4 Phase 2*	*B4 Phase 3*
0.121	q_1^a	3.78×10^7	100		
0.143	q_1^b	2.02×10^8		001	
0.153	q_2^a	3.64×10^9	001		
0.172	q_1^c	1.09×10^8			001
0.209	q_3^a	4.39×10^7	101		
0.241	q_4^a	4.74×10^7	200		
0.287	q_2^b	6.57×10^7		002	
0.304	q_5^a	7.59×10^7	002		
0.342	q_2^c	4.03×10^7			002
0.360	q_6^a	1.790×10^7	300		
0.429	q_3^b	1.45×10^7		003	
0.524	q_3^c	1.17×10^7			003
0.576	q_4^b	1.31×10^7		004	
0.72	q_5^b	3.13×10^5		005	

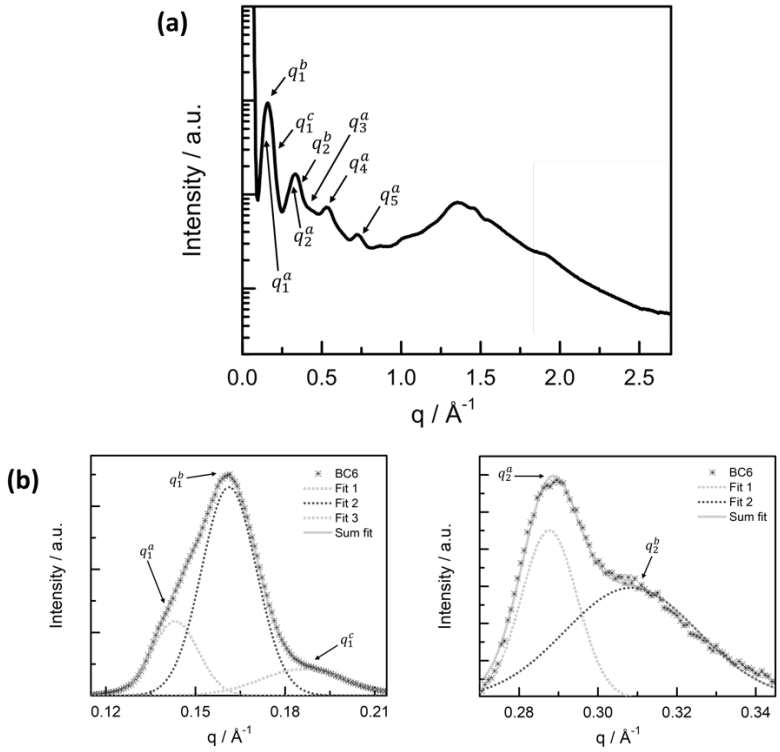

Fig. S29. (a) XRD analysis data showing intensity (a.u.) vs. wave vector q (Å^{-1}) of the combined MAXD-WAXS region for **BC6** taken after slow cooling from the isotropic liquid phase at room temperature. (b) Peak deconvolution; for data see Table S14.

Table S14. Peak positions, assignment, relative intensity values, and Miller indices for the three B4 structures formed by **BC6** upon slow cooling.

q/Å^{-1}	*Assignment*	*Relative Intensity*	*Index*		
			B4 Phase 1	*B4 Phase 2*	*B4 Phase 3*
0.143	q_1^a	8.67×10^8	001		
0.159	q_1^b	1.79×10^9		001	
0.185	q_1^c	2.93×10^8			001
0.287	q_2^a	9.12×10^7	002		
0.31	q_2^b	6.10×10^7		002	
0.426	q_3^a	2.34×10^7	003		
0.56	q_4^a	2.34×10^7	004		
0.72	q_5^a	3.74×10^7	005		

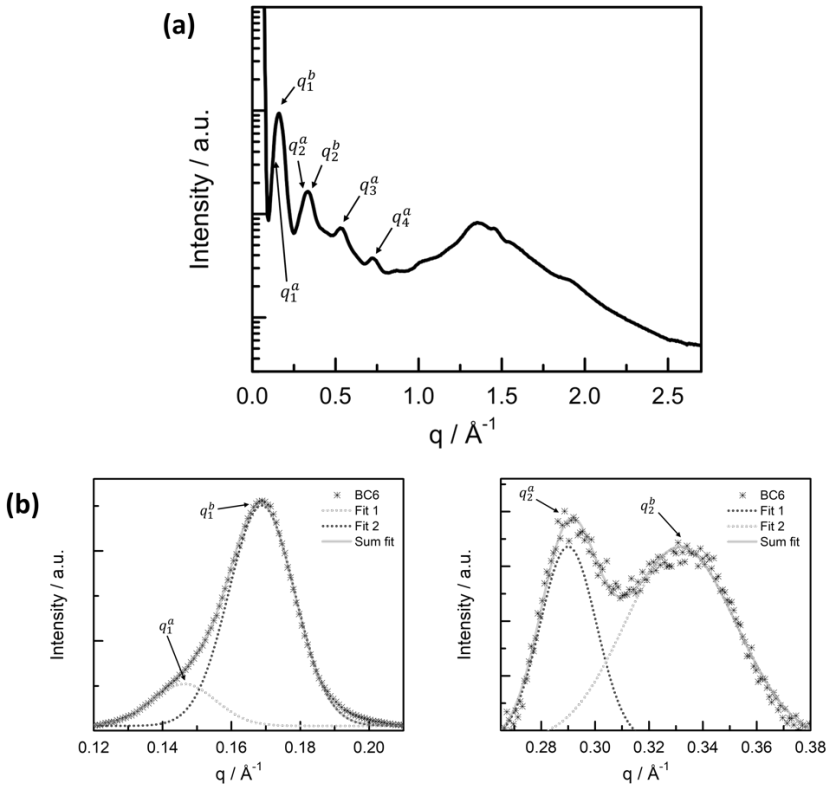

Fig. S30. (a) XRD analysis data showing intensity (a.u.) vs. wave vector q ($Å^{-1}$) of the combined MAXD-WAXS region for **BC6** taken after rapid cooling from the isotropic liquid phase at room temperature. (b) Peak deconvolution; for data see Table S15.

Table S15. Peak positions, assignment, relative intensity values, and Miller indices for the two B4 structures formed by **BC6** upon rapid cooling.

$q/Å^{-1}$	*Assignment*	*Relative Intensity*	*Index*	
			B4 Phase 1	*B4 Phase 2*
0.146	q_1^a	3.07×10^8	001	
0.169	q_1^b	1.32×10^9		001
0.291	q_2^a	4.86×10^7	002	
0.332	q_2^b	4.08×10^7		002
0.432	q_3^a	1.94×10^7	003	
0.57	q_4^a	1.86×10^7	004	

References

(S1) L. Li, M. Salamończyk, A. Jákli, T. Hegmann, *Small*, 2016, **12**, 3944.

(S2) L. Li, M. Salamończyk, S. Shadpour, C. Zhu, A. Jákli, T. Hegmann, *Nat. Commun.*, 2018, **9**, 714.

(S3) S. Shadpour, A. Nemati, N. J. Boyd, L. Li, M. E. Prévôt, S. L. Wakerlin, J. P. Vanegas, M. Salamończyk, E. Hegmann, C. Zhu, M. R. Wilson, A. I. Jákli, T. Hegmann, *Mater. Horizons*, 2019, **6**, 959.

(S4) S. Shadpour, A. Nemati, M. Salamończyk, M. E. Prévôt, J. Liu, N. J. Boyd, M. R. Wilson, C. Zhu, E. Hegmann, A. I. Jákli, T. Hegmann, *Small*, 2020, **16**, 1905591.